*Human Molecular Genetics*, 2017, Vol. 26, No. 20 3973–3988

**doi: 10.1093/hmg/ddx284**
Advance Access Publication Date: 18 July 2017
Original Article

ORIGINAL ARTICLE

# Enhanced tau pathology via RanBP9 and Hsp90/Hsc70 chaperone complexes

Jung A. Woo[1,2,*], Tian Liu[1,2], Xingyu Zhao[1,2], Courtney Trotter[1,2], Ksenia Yrigoin[1], Sara Cazzaro[1], Emilio De Narvaez[1], Hirah Khan[1], Richard Witas[1], Anusha Bukhari[1], Kamal Makati[1], Xinming Wang[1,3], Chad Dickey[1,2,4] and David E. Kang[1,2,4,*]

[1]USF Health Byrd Alzheimer's Institute, [2]Department of Molecular Medicine, [3]Department of Molecular Pharmacology and Physiology, University of South Florida, Morsani College of Medicine, Tampa, FL 33613, USA and [4]James A. Haley Veteran's Administration Hospital, Research Division, Tampa, FL 33612, USA

*To whom correspondence should be addressed. Tel: 858-717-1456; Email: jwoo1@health.usf.edu (J.A.W.), Tel: 858-519-7081; Email: dkang@health.usf.edu (D.E.K.)

## Abstract

Accumulation of amyloid β (Aβ) and tau represent the two major pathological hallmarks of Alzheimer's disease (AD). Despite the critical importance of Aβ accumulation as an early event in AD pathogenesis, multiple lines of evidence indicate that tau is required to mediate Aβ-induced neurotoxic signals in neurons. We have previously shown that the scaffolding protein Ran-binding protein 9 (RanBP9), which is highly elevated in brains of AD and AD mouse models, both enhances Aβ production and mediates Aβ-induced neurotoxicity. However, it is unknown whether and how RanBP9 transmits Aβ-induced neurotoxic signals to tau. Here we show for the first time that overexpression or knockdown of RanBP9 directly enhances and reduces tau levels, respectively, *in vitro* and *in vivo*. Such changes in tau levels are associated with the ability of RanBP9 to physically interact with tau and heat shock protein 90/heat shock cognate 70 (Hsp90/Hsc70) complexes. Meanwhile, both RanBP9 and tau levels are simultaneously reduced by Hsp90 or Hsc70 inhibitors, whereas overexpression or knockdown of RanBP9 significantly diminishes the anti-tau potency of Hsp90/Hsc70 inhibitors as well as Hsc70 variants (WT & E175S). Further, RanBP9 increases the capacity for Hsp90 and Hsc70 complexes to bind ATP and enhances their ATPase activities *in vitro*. These observations *in vitro* and cell lines are recapitulated in primary neurons and *in vivo*, as genetic reduction in *RanBP9* not only ameliorates tauopathy in Tau-P301S mice but also rescues the deficits in synaptic integrity and plasticity.

## Introduction

The major pathological hallmarks of Alzheimer's disease (AD) are the accumulation of amyloid β (Aβ) and hyperphosphorylated tau in senile plaques and neurofibrillary tangles, respectively, associated with mitochondrial and synaptic dysfunction, cytoskeletal aberrations, and neuroinflammation. Recent studies have demonstrated that Aβ-induced neurotoxic signals are ultimately transmitted via tau since the loss of tau abrogates many deleterious effects of Aβ-induced mitochondrial/synaptic dysfunction and cognitive impairments (1–3). Therefore, identification of upstream and downstream intermediates of Aβ- and phospho-tau-induced neurotoxic mechanisms are critically important to understand underlying pathological pathways in AD.

The microtubule-associated protein (MAP) tau, which functions to stabilize microtubules (MTs), is an intrinsically disordered protein that promotes tauopathy via its post-translational modification and abnormal accumulation (4–6). Multiple studies have shown that tau stability is highly dependent on molecular

**Received:** April 28, 2017. **Revised:** July 4, 2017. **Accepted:** July 14, 2017

chaperons such as heat shock protein 90 (Hsp90) and heat shock protein 70 (Hsp70), two major molecular chaperones that affect tau misfolding, self-aggregation, and clearance (7–11). While Hsp90, the most abundant chaperone protein in neurons, is known to refold or degrade various aberrant misfolded proteins, it also has been associated with preserving aberrant tau. Indeed, it has been reported that various Hsp90 inhibitors lead to the degradation of abnormal tau and reduced tauopathy (9,12). It has also been shown that heat shock cognate 70 (Hsc70), a constitutively expressed Hsp70 isoform, also preserves aberrant tau levels upon microtubule destabilization (10). Accordingly, several Hsc70 inhibitors have also shown to decrease tau levels *in vitro* and *in vivo* (11,13–15).

We have previously shown that the scaffolding protein, Ran-binding protein 9 (RanBP9), is significantly increased in the brains of AD patients and the APP transgenic mouse models (16–18). Furthermore, we found that RanBP9 promotes Aβ production by enhancing the endocytosis of the amyloid precursor protein (APP) by scaffolding APP/BACE1 complexes while simultaneously promoting Aβ-induced neurotoxicity by disrupting integrin-dependent focal adhesion complexes and inducing mitochondrial dysfunction (17–21). Given that tau is ultimately required to transmit Aβ-induced neurotoxic signals to induce synaptic/mitochondrial dysfunction and cognitive impairment (22,23), we hypothesized that RanBP9 functions as an integral intermediate that also promotes tauopathy. In this study, we show for the first time that RanBP9 increases tau levels by promoting tau/Hsp90/Hsc70 complexes and that genetic reduction in *RanBP9* significantly mitigates tauopathy, gliosis, and synaptic dysfunction associated with Tau-P301S transgenic mice.

## Results

### Endogenous RanBP9 regulates tau levels without altering tau mRNA

To determine whether the scaffolding protein RanBP9 plays a role in the regulation of tau, we first used HeLa cells stably transfected with V5-tagged human 4R0N tau (Hela V5-Tau). In these cells, we transfected control or RanBP9 siRNA to biochemically assess total and phospho-tau levels. Surprisingly, knockdown of endogenous RanBP9 by siRNA significantly reduced both total tau (Tau46 antibody) and phospho-tau (PHF1 antibody) concomitant with a reduction in RanBP9 (Fig. 1A and B). Next, we next cultured cortical primary neurons derived from wild type (WT), Tau-P301S (PS19) (24), and Tau-P301S transgenic mice with hemizygous *RanBP9* deficiency (Tau-P301S;*RanBP9*+/−). Indeed, we observed an increase in total tau (Tau46) and PHF1-tau in Tau-P301S transgenic neurons, which were significantly reversed in littermate Tau-P301S;*RanBP9*+/− neurons on DIV14 (Fig. 1C and D). Both the upper transgenic tau and lower endogenous tau bands were reduced by *RanBP9* genetic reduction, and *RanBP9*+/− neurons consistently demonstrated a 50–70% reduction in endogenous RanBP9 (Fig. 1C) as we previously demonstrated (17–19). To ascertain this result in a different way in primary neurons, DIV21 neurons were stained for total tau (Tau5 antibody). Quantification of tau intensity in primary neurites indeed confirmed that tau levels were increased in Tau-P301S neurons compare to WT littermate neurons, whereas Tau-P301S;*RanBP9*+/− neurons demonstrated a significant reduction in tau intensity (Fig. 1E and F), indicating that endogenous RanBP9 increases tau levels in cell lines and in primary neurons.

We next examined whether RanBP9 alters tau protein levels at the level of tau mRNA. To this end, we first performed quantitative RT-PCR (qRT-PCR) to monitor human tau mRNA levels in brains 5-month old Tau-P301S and Tau-P301S;*RanBP9*+/− mice. We observed no differences in relative human tau mRNA levels between the genotypes (Fig. 1G). Furthermore, we found no significant differences in endogenous mouse tau mRNA levels in brains of 5-month-old WT, Tau-P301, Tau-P301S;*RanBP9*+/−, and *RanBP9*+/− littermates by qRT-PCR (Fig. 1H). To ensure that these results from the brain are also consistent in primary neurons, we also utilized hippocampal primary neurons from WT and *RanBP9*+/− mice. As expected, we also found no significant differences in mouse tau mRNA levels between WT vs *RanBP9*+/− primary neurons on DIV14 (Fig. 1I), collectively indicating that RanBP9 does not alter tau protein levels by regulating tau mRNA.

As RanBP9 positively regulates Aβ secretion (19,20), it is possible that alterations in Aβ by RanBP9 might influence tau levels. To determine whether Aβ plays a role in RanBP9-induced changes in tau, we treated Hela V5-tau cells transfected with RanBP9 siRNA with/without the potent γ-secretase inhibitor DAPT. As expected, RanBP9 knockdown significantly reduced tau levels, whereas DAPT treatment had no effect on tau levels despite an expected increase in APP C-terminal fragment (CTF) (Fig. 1J and K). To ensure that these results are consistent in primary neurons, we utilized cortical primary neurons derived from Tau-P301S and Tau-P301S;*RanBP9*+/− mice. As expected, Tau-P301S;*RanBP9*+/− primary neurons showed significantly decreased tau level compared to Tau-P301S littermates, whereas γ-secretase inhibition (DAPT) again had no effect on tau levels. These data indicate that the observed changes in tau levels by RanBP9 are independent of its effects on Aβ (Fig. 1l and M).

### RanBP9 interacts with tau and Hsp90/Hsc70 complexes to increase tau levels

We next sought to explore the underlying mechanistic relationship between RanBP9 and tau at the post-translational level. RanBP9 is a multimeric scaffolding protein (25), which we have previously shown to enhance APP and BACE1 complexes to increase APP endocytosis and Aβ production (19). RanBP9 has also been shown to alter the action of Hsp90 on c-raf (26). Given that Hsp90/Hsc70 complexes are well known to enhance tau stability at the protein level (7–9,14,15,27–30), we hypothesized that RanBP9 may play a role in regulating tau levels via molecular chaperones such as Hsp90 and/or Hsc70. To this end, we first assessed whether RanBP9 overexpression affects the interaction between tau and Hsp90 in Hela V5-Tau cells by co-immunoprecipitation (IP) experiments. RanBP9 overexpression significantly increased the amount of endogenous Hsp90 in tau immune complexes, whereas little to no Hsp90 or RanBP9 were detected in IgG-bead immune complexes alone (Fig. 2A and B). We also observed the presence of endogenous RanBP9 in tau immune complexes, which increased upon RanBP9 transfection (Fig. 2A) Conversely, siRNA knockdown of RanBP9 significantly reduced endogenous Hsp90 in tau immune complexes (Fig. 2C and D). Likewise in brain, we found that Hsp90/tau complexes were significantly reduced in 5-month-old Tau-P301S;*RanBP9*+/− hippocampus compare to Tau-P301S littermates (Fig. 2E and F). RanBP9 was also observed in tau immune complexes in WT brains, which increased in Tau-P301S mice (Fig. 2E and F). Again, neither Hsp90 nor RanBP9 was detected in IgG-bead immune complexes alone (Fig. 2E). Nearly identical findings were also observed in DIV18 cortical neurons, in which the Hsp90/tau complex was significantly reduced by genetic reduction of

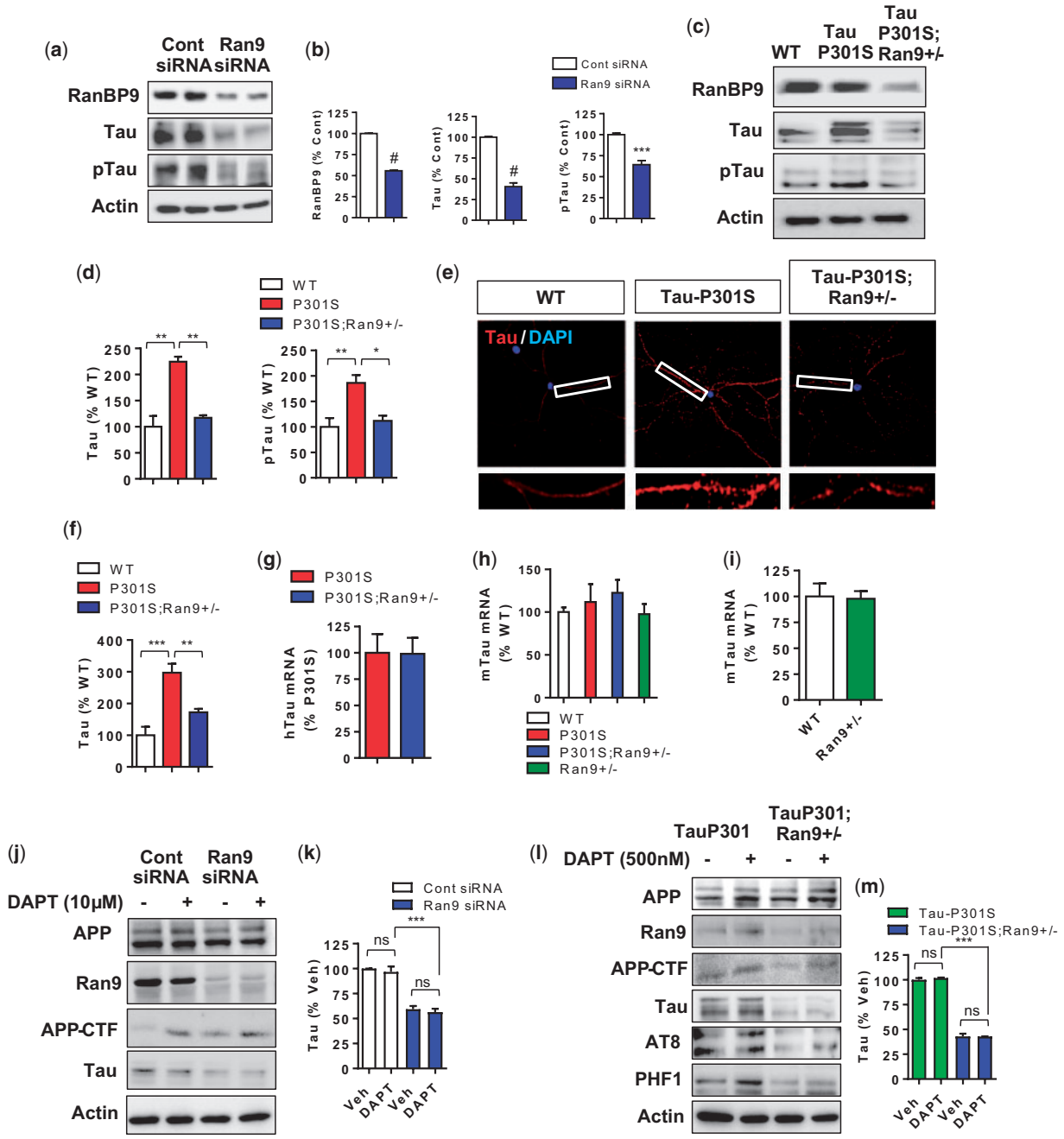


**Figure 1.** RanBP9 increases tau protein levels without altering tau mRNA. (**A,B**) HeLa cells stably expressing V5-tagged 4R0N tau (HeLa V5-Tau) transiently transfected with control siRNA or RanBP9 siRNA, and equal protein amounts subjected to immunoblotting for RanBP9, total tau (tau46), and p-tau (PHF1). Representative blots shown. (**B**) Quantification of RanBP9, total tau (tau46), and pTau (PHF1) levels following control siRNA or RanBP9 siRNA transfection (t-test,$^{***}P < 0.0005$, $^{\#}P < 0.0001$, $n = 4$ replicates). (**C,D**) DIV14 cortical primary neurons from WT, TauP301S, and TauP301S;*RanBP9*+/− subjected to immunoblotting for the indicated proteins. Representative blots shown. (**D**) Quantification of total tau (tau46) and p-tau (PHF1) levels from cortical primary neurons (1-way ANOVA, post hoc Tukey, $^{*}P < 0.05$, $^{**}P < 0.005$, $n = 3$ replicates). (**E,F**) DIV21 hippocampal neurons from WT, Tau-P301S and Tau-P301S;*RanBP9*+/− mice stained for total tau (Tau5). Representative images and magnified bottom insets shown. (**F**) Quantification of tau intensity in WT, Tau-P301S and Tau-P301S;*RanBP9*+/− neurons (1-way ANOVA, post hoc Tukey, $^{**}P < 0.005$, $^{***}P < 0.0005$, $n = 5$–6 replicates). (**G**) Quantification of human tau mRNA levels by qRT-PCR from brains of 5-month-old Tau-P301S and Tau-P301S;*RanBP9*+/− littermates (t-test, not significant, $n = 4$ mice per genotype). (**H**) Quantification of mouse tau mRNA by qRT-PCR from brains of 5-month-old WT, Tau-P301S, Tau-P301S;*RanBP9*+/−, and *RanBP9*+/− littermates (1-way ANOVA, not significant, $n = 4$ mice per genotype). (**I**) Quantification of mouse tau mRNA by qRT-PCR from DIV21 cortical primary neurons derived from WT and *RanBP9*+/− littermates (t-test, not significant, $n = 4$ mice per genotype). All error bars represent S.E.M. (**J**) HeLa V5-Tau cells transiently transfected with control siRNA or RanBP9 siRNA and treated with/without DAPT (10 μM) for 24 h. Equal protein amounts subjected to immunoblotting for APP, RanBP9, APP-CTF, and tau. (**K**) Quantification of total tau levels following control siRNA or RanBP9 siRNA transfection (1-way ANOVA, post hoc Tukey, $^{***}P < 0.0005$, $n = 4$ replicates). (**L**) DIV14 cortical primary neurons from Tau-P301S and Tau-P301S;*RanBP9*+/− mice treated with/without DAPT 500 nM for 24 h and equal protein amounts subjected to immunoblotting for indicated proteins. (**M**) Quantification of total tau levels from cortical primary neurons (1-way ANOVA, post hoc Tukey, $^{***}P < 0.0005$, $n = 4$ replicates).

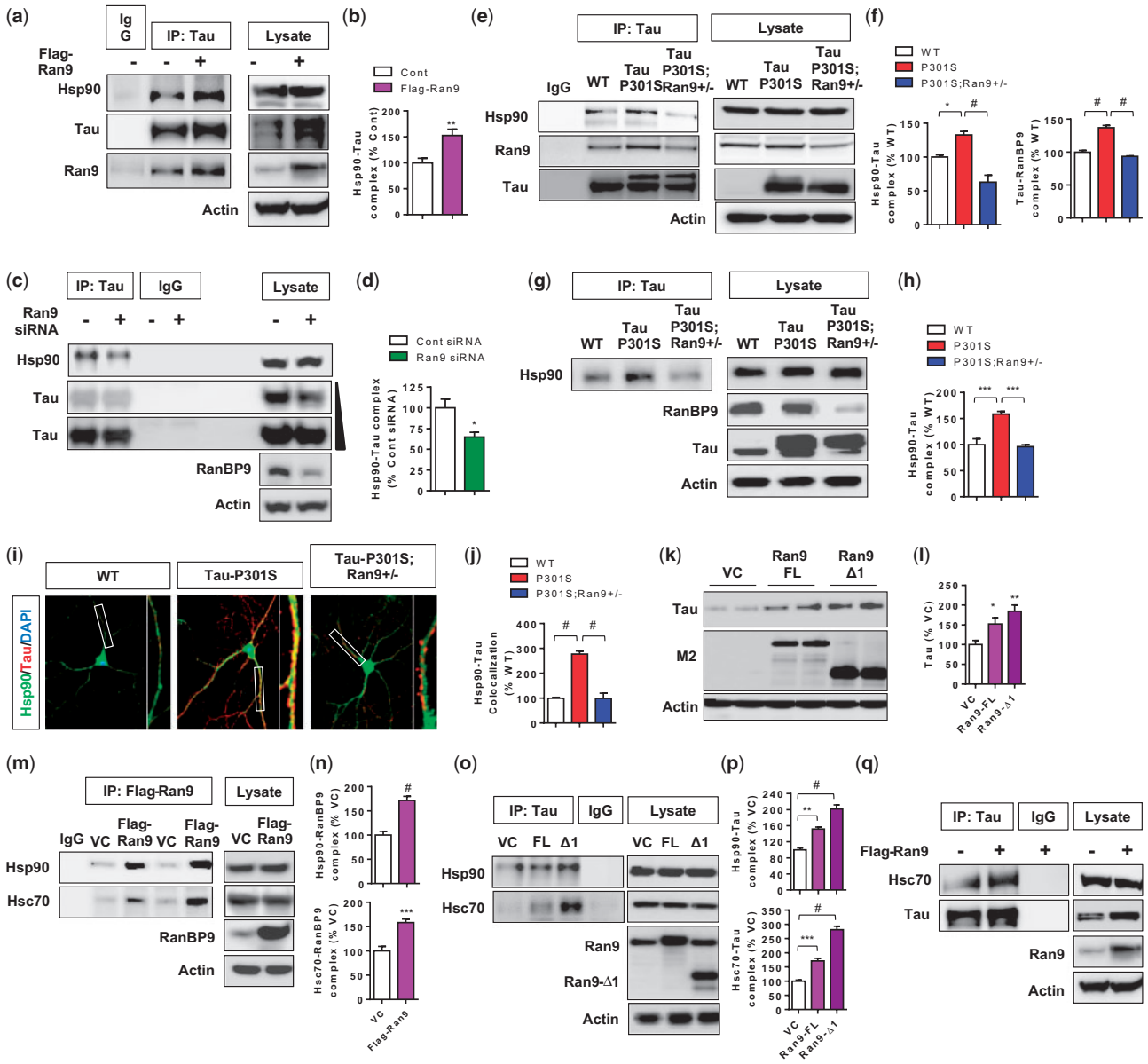


**Figure 2.** RanBP9 interacts with tau andHsp90/Hsc70 complexes to increase tau levels. (**A,B**) Hela V5-Tau cells transfected with vector control or RanBP9, immunoprecipitated (IP) for tau or IgG beads alone, and immunoblotted for Hsp90 and tau. Same lysates also immunoblotted for Hsp90, tau, RanBP9, and actin. (**B**) Quantification of Hsp90 in tau complexes (t-test, $^{**}P < 0.005$, $n = 8$ replicates). (**C,D**) Hela V5-Tau cells transfected with control or RanBP9 siRNA, IPed for tau or IgG beads alone, and immunoblotted for Hsp90 and tau. Same lysates also immunoblotted for Hsp90, tau, RanBP9, and actin. (**D**) Quantification of Hsp90 in tau complexes (t-test, $^{*}P < 0.05$, $n = 5$ replicates). (**E,F**) Brain lysates from 5-month-old WT, Tau-P301S, and Tau-P301S;*RanBP9*+/− IPed for tau or IgG beads alone and immunoblotted for Hsp90, RanBP9, and tau. Lysates also immunoblotted for Hsp90, RanBP9, tau, and actin. (**F**) Quantification of Hsp90 in tau complexes (1-way ANOVA, post hoc Tukey, $^{*}P < 0.05$, $^{\#}P < 0.0001$, $n = 6$ mice/genotype). (**G,H**) DIV18 cortical neurons derived from WT, Tau-P301S, and Tau-P301S;*RanBP9*+/− mice were IPed for tau and immunoblotted for Hsp90. Lysates also immunoblotted for Hsp90, RanBP9, tau, and actin. (**H**) Quantification of Hsp90 in tau complexes (1-way ANOVA, post hoc Tukey, $^{***}P < 0.0005$, $n = 4$ mice/genotype). (**I,J**) DIV21 hippocampal primary neurons derived from WT, Tau-P301S, and Tau-P301S;*RanBP9*+/− mice subjected to staining for Hsp90 and tau. Representative images and magnifications of primary neurites (right panels) shown). (**J**) Quantification of Hsp90 colocalized with tau (1-way ANOVA, post hoc Tukey, $^{\#}P < 0.0001$, $n = 4$–6 replicates/genotype). (**K,L**) Hela V5-Tau cell transfected with vector control (VC), Flag-RanBP9, or Flag-RanBP9-Δ1 and immunoblotted for tau, M2 flag, and actin. (**L**) Quantification of tau levels (1-way ANOVA, posthoc Tukey, $^{*}P < 0.05$, $^{**}P < 0.005$, $n = 5$ replicates). (**M,N**) Hela V5-Tau cells transfected with VC or Flag-RanBP9, IPed for RanBP9 or IgG beads alone, and immunoblotted for Hsp90 and Hsc70. Lysates also immunoblotted for Hsp90, Hsc70, M2, RanBP9, and actin. (**N**) Quantification of Hsp90 and Hsc70 in RanBP9 complexes (t-test, $^{\#}P < 0.0001$, $^{***}P < 0.0005$, $n = 7$ replicates). (**O,P**) Hela V5-Tau cells transfected with VC, Flag-RanBP9, or Flag-RanBP9-Δ1; IPed for tau or IgG beads alone, and immunoblotted for Hsp90, Hsc70, and tau. Lysates also immunoblotted forHsp90, Hsc70, RanBP9, and actin. (**P**) Quantification of Hsp90 and Hsc70 in tau complexes (1-way ANOVA, posthoc Tukey, $^{**}P < 0.005$, $^{***}P < 0.0005$, $^{\#}P < 0.0001$, $n = 4$–6 replicates). (**Q**) Hela V5-Tau cells transfected with VC or Flag-RanBP9, IPed for tau, and immunoblotted for Hsc70 and tau. Lysates also immunoblotted for Hsp90, Hsc70, RanBP9, and actin. Note the increase in total tau and tau/Hsc70 complex upon RanBP9 transfection.

*RanBP9* (Fig. 2G and H). In all cases in Hela V5-Tau cells, primary neurons, or brain, we did not observe differences in Hsp90 levels secondary to changes in RanBP9 expression. To assess this phenotype in a different way, we performed tau/Hsp90 double immunocytochemistry in DIV21 hippocampal primary neurons, which consistently showed that the colocalization of tau with Hsp90 in primary neurites was significantly reduced in Tau-P301S;*RanBP9*+/− neurons compared to Tau-P301S littermate

neurons (Fig. 2I and J), collectively demonstrating that RanBP9 enhances the Hsp90/tau complex.

Consistent with the aforementioned observations, overexpression of Flag-RanBP9 or Flag-RanBP9-Δ1 deletion mutant in Hela V5-Tau cells significantly increased tau levels (Fig. 2K and L). The RanBP9-Δ1 (residues 1-392) mutant retains the proline-rich (PRD), PTPN13-Like Y-linked- in splA kinase and ryanodine receptor (PRY-SPRY) and lissencephaly homology (LisH) domains but lacks the C-terminal CTLH and CRA domains. This N-terminal fragment of RanBP9 has previously been shown to strongly enhance Aβ production by scaffolding APP/BACE-1 complexes together and is significantly increased in the brains of AD patients (16,19). Given that RanBP9 formed a complex with tau and promoted the formation of Hsp90/tau and complexes, we next tested whether RanBP9 *per se* interacts with Hsp90 and/or Hsc70 complexes, the latter due to the mutual cooperation of Hsp90/Hsc70 complexes in tau preservation. Indeed, both Hsp90 and Hsc70 were detected in RanBP9 immune complexes, and overexpression of RanBP9 in Hela V5-Tau cells significantly enhanced both Hsp90 and Hsc70 in RanBP9 immune complexes (Fig. 2M and N). This association of RanBP9 with Hsp90 and Hsc70 were not dependent on tau overexpression, as RanBP9/Hsp90 and RanBP90/Hsc70 complexes were similarly detected in Hela cells lacking tau expression (Supplementary Material, Fig. S1). In Hela-V5-Tau cells, overexpression of RanBP9 or RanBP9-Δ1 mutant significantly increased the amount of Hsp90 and Hsc70 in tau immune complexes, with the RanBP9-Δ1 mutant having a stronger effect than full-length RanBP9 (Fig. 2O and P). However, the RanBP9-Δ1 L mutant (residues 1-340), which is the Δ1 lacking the LisH dimerization domain (16), did not effectively increase Hsp90/Hsc70 complexes with tau nor increase tau levels (Supplementary Material, Fig. S2), suggesting a role for RanBP9 dimerization/oligomerization in this activity. Concomitant with an increase in tau/Hsc70 complexes upon RanBP9 overexpression, the amount of tau pulled down in tau immune complexes was also expectedly increased, reflecting an increase in total tau (Fig. 2Q). Finally, we confirmed in cell-free recombinant protein pulldown assays that recombinant RanBP9 PRY-SPRY-LisH (PSL) domain (residues 147-397) directly binds to recombinant Hsp90, Hsc70, and tau, and that RanBP9-PSL also increases the tau/Hsp90 complex *in vitro* (Supplementary Material, Fig. S3). These data collective indicate that RanBP9 directly forms complexes with tau and Hsp90/Hsc70 to promote the stability of tau.

## Hsp90/Hsc70 inhibitors reduce both tau and RanBP9 level in cell lines and primary neurons

Multiple studies have shown that inhibitors of the ATPase activity of Hsp90 or Hsc70 ameliorate tauopathies by reducing tau levels (9,12,15,27,28,31). Given that Hsp90 and Hsc70 formed complexes not only with tau but also with RanBP9, we assessed the effects of various Hsp90 and Hsc70 inhibitors simultaneously on tau and RanBP9 protein levels. First, we treated Hela V5-Tau cells with 17-AAG, a well-characterized Hsp90 inhibitor. As expected, 17-AAG (1 μM) treatment for 16 h significantly reduced tau levels by ∼50% (Fig. 3A and B). Surprisingly, we also noticed that RanBP9 levels were equally reduced by 17-AAG treatment (Fig. 3A and B). To confirm our findings, we treated DIV15 primary cortical neurons with 17-AAG. Consistently, 17-AAG treatment to primary neurons equally reduced both tau and RanBP9 levels (Fig. 3C and D). Next, we tested a novel, novobiocin-based Hsp90 inhibitor KU-32 (32) in Hela V5-Tau cells. Consistent with 17-AAG treatment, KU-32 treatment significantly reduced both tau and RanBP9 levels (Fig. 3E and F). Again in DIV15 primary cortical neurons, KU-32 treatment dose-dependently decreased tau and RanBP9 levels, the latter even more effectively than tau (Fig. 3G and H). To examine the effect of Hsc70 inhibition on RanBP9 and tau levels, we used JG-98, an allosteric Hsc70 inhibitor (33), which has been shown to exert higher anti-tau capacity compared to other compounds (11,13,15,34,35). In DIV15 primary neurons, treatment of JG-98 dose-dependently reduced both tau and RanBP9 levels by ∼50% and ∼70%, respectively, at 10 μM concentration (Fig. 3I and J). To determine whether the ATPase activities of Hsp90/Hsc70, which govern tau stability, also alter RanBP9 levels, we transfected Hela V5-Tau cells with the Hsp90 dominant negative variant (Hsp90 D88N), which does not hydrolyze ATP (36). Indeed, Hsp90 dominant negative transfection significantly reduced endogenous RanBP9 levels (Fig. 3K and L). Likewise, the Hsc70 dominant negative variant (Hsc70 E175S) (11,37) also significantly reduced endogenous RanBP9 levels (Fig. 3M and N) Thus, Hsp90/Hsc70 inhibitors as well as Hsp90/Hsc70 dominant negative variants decrease both tau and RanBP9 levels.

## RanBP9 modulates the efficacy of Hsp90/Hsc70 inhibitors and Hsc70 variants

Given that Hsp90/Hsc70 inhibitors decreased both tau and RanBP9, we next hypothesized that Hsp90/Hsc70 inhibitors reduce tau at least in part via RanBP9. Thus, we examined whether modulating RanBP9 levels alters the efficacy of Hsp90/Hsc70 inhibitors. As expected, RanBP9 overexpressing cells showed increased tau levels (Fig. 4A and B). However, the efficacy of 17-AAG was significantly reduced by RanBP9 overexpression (Fig. 4A and B). Conversely, RanBP9 siRNA knockdown significantly reduced tau levels (Fig. 4C and D). However, the efficacy of 17-AAG likewise was significantly nullified by RanBP9 knockdown (Fig. 4C and D), such that 17-AAG no longer produced a significant reduction in tau under these conditions. We next assessed the efficacy of another Hsp90 inhibitor KU-32 with or without RanBP9 knockdown in Hela V5-Tau cells. While KU-32 reduced tau levels in a dose-dependent manner in control siRNA transfected cells, RanBP9 siRNA transfected cells already showed significantly reduced tau levels, and KU-32 treatment produced no significant effects on tau levels upon RanBP9 siRNA transfection (Fig. 4E and F). Furthermore, we monitored the efficacy of the Hsc70 inhibitor JG-98 with or without RanBP9 knockdown in Hela V5-Tau cells. As expected, RanBP9 siRNA knockdown significantly reduced tau levels. Whereas JG-98 treatment robustly reduced tau in control cells, the same treatment failed to reduce tau in RanBP9 siRNA transfected cells (Fig. 4G and H), suggesting that the interaction of RanBP9 with Hsp90/Hsc70 complexes effectively modifies their ability to preserve tau.

Previous studies have shown that while Hsc70 stabilizes tau, the Hsc70 variant E175S, which does not have Hsc70 activity but still binds to tau, fails to increase tau and often reduces tau in a dominant negative manner (11,37). In our studies, we observed that Hsc70 overexpression in Hela V5-Tau cells significantly increased tau levels, whereas Hsc70-E175S expression failed to increase tau (Fig. 4I and J). To this end, we used these Hsc70 variants to study the effects of RanBP9 on tau without using drug inhibitors. As expected, expression of RanBP9-Δ1 increased

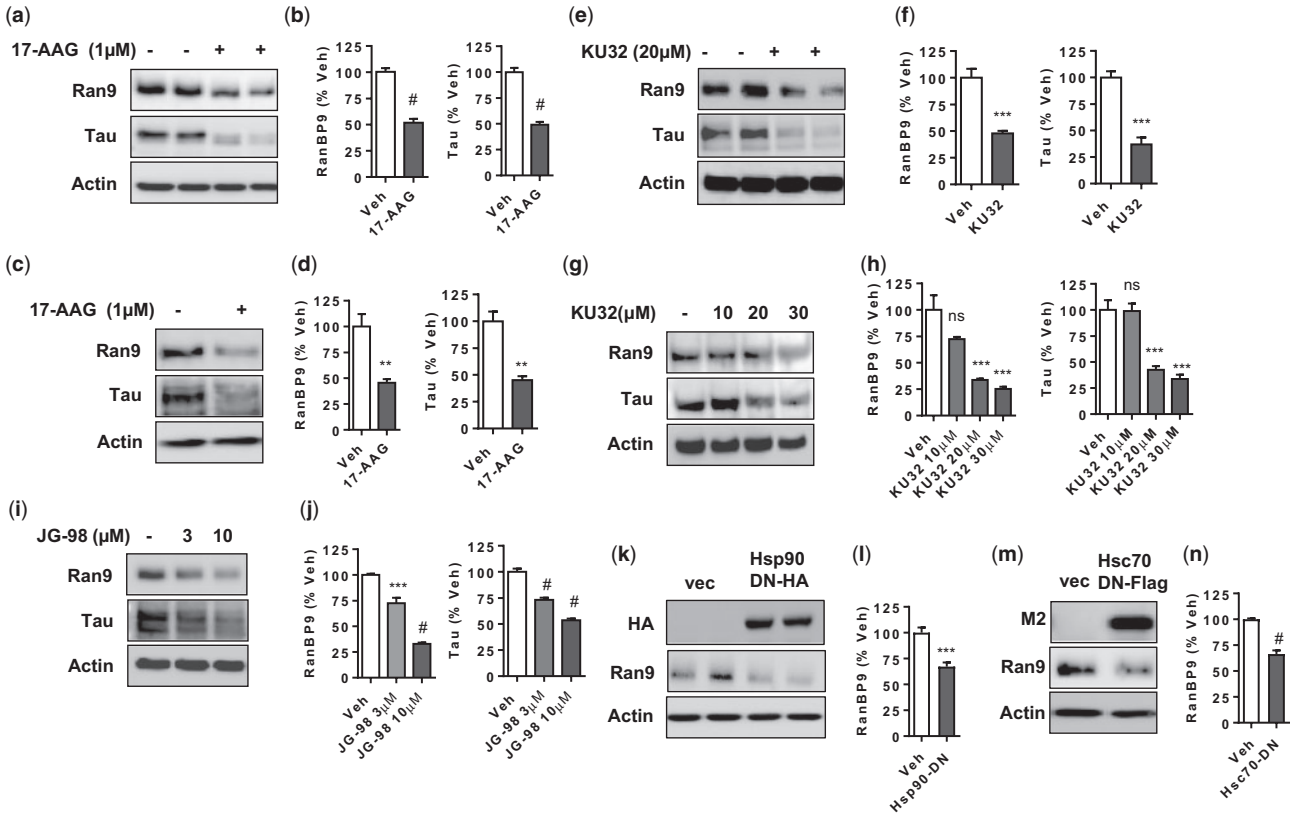


**Figure 3.** Co-regulation of tau and RanBP9 levels by Hsp90/Hsc70 inhibitors and modulation of inhibitor efficacy by RanBP9. (**A,B**) Hela V5-Tau cells treated with/without 17-AAG (1 μM) for 16 h and subjected to immunoblotting for the indicated proteins. (**B**) Quantification of RanBP9 and tau levels. (t-test, $^{\#}P < 0.0001$, $n = 6$ replicates). (**C,D**) DIV15 cortical primary neurons treated with/without 17-AAG (1 μM) for 16 h and subjected to immunoblotting for the indicated proteins. (**D**) Quantification of RanBP9 and tau levels (t-test, $^{**}P < 0.005$, $n = 6$ replicates). (**E,F**) Hela V5-Tau cells treated with/without KU-32 (20 μM) for 16 h and subjected to immoblotting for the indicated proteins. (F) Quantification of RanBP9 and tau levels with/without KU-32 (t-test, $^{***}P < 0.0005$, $n = 6$ replicates). (**G,H**) DIV15 cortical primary neurons treated with the indicated concentrations of KU-32 and subjected to immunoblotting for the indicated proteins. (**H**) Quantification of RanBP9 and tau levels (1-way ANOVA, post hoc Tukey, $^{***}P < 0.0005$, $n = 6$ replicates). (**I,J**) DIV15 cortical primary neurons treated with the indicated concentrations of JG-98 for 1 h. (**J**) Quantification of RanBP9 and tau levels (1-way ANOVA, post hoc Tukey, $^{***}P < 0.0005$, $n = 6$ replicates). (**K**) Hela V5-Tau cells transfected with VC or Hsp90 dominant negative variant (Hsp90 D88N) and immunoblotted for HA, RanBP9, and actin. (**L**) Quantification of RanBP9 levels (t-test, $^{***}P < 0.0005$, $n = 4$ replicates). (**M**) Hela V5-Tau cells transfected with VC or Hsc70 dominant negative variant (Hsc70 E175S) and immunoblotted for M2, RanBP9, and actin. (**N**) Quantification of RanBP9 levels (t-test, $^{***}P < 0.0005$, $n = 6$ replicates).

tau levels by more than 60% (Fig. 4I and J). However, similar to that seen with Hsp90 and Hsc70 inhibitors, expression of Hsc70 variants (WT or E175S) had no significant effects on tau levels when co-transfected with RanBP9-Δ1 (Fig. 4I and J). We next tested whether genetic reduction in *RanBP9* also alters the effects of Hsc70 variants in cortical primary neurons. Upon transduction of Tau-P301S neurons with control adeno-associated virus 9 (AAV9), Hsc70-AAV9, or Hsc70-E175S-AAV9, we again observed an increase in tau levels by Hsc70 but not Hsc70-E175S transduction (Fig. 4K and L). However, transduction of Hsc70 variants did not significantly alter tau levels in Tau-P301S;*RanBP9*+/− neurons (Fig. 4K and L). To confirm this observation in a different way, we transduced WT and *RanBP9*−/− hippocampal neurons with Hsc70 or Hsc70-E175S AAV9 on DIV7 and performed immunocytochemistry for tau on DIV21. As expected, tau intensity was significantly increased by Hsc70 transduction in WT neurons, whereas Hsc70-E175S transduction somewhat reduced tau levels (Fig. 4M and N). In contrast, tau intensity was modestly but significantly reduced by Hsc70 transduction in *RanBP9*−/− neurons, whereas Hsc70-E175S transduction had no effect on tau levels in *RanBP9*−/− neurons (Fig. 4M and N). Likewise, the efficacies of the Hsp90 inhibitor 17-AAG (Fig. 4O and P) and the Hsc70 inhibitor JG-98 (Fig. 4Q and R) were effectively diminished in *RanBP9*−/− primary neurons, confirming the prediction that Hsp90/Hsc70 complexes work in concert with RanBP9 to preserve tau.

## RanBP9 promotes ATP-binding ability of Hsp90/Hsc70 complexes and increases Hsc70 ATPase activity

Previous studies have shown that inhibitors of ATP binding or ATPase activity can block Hsp90 function as well as reduce tau phosphorylation and protein levels (9,12). To determine whether RanBP9 affects the ATP-binding ability of Hsp90, we performed an ATP-agarose pull down assay using cell lysates from Hela V5-Tau cells transfected with vector control, an irrelevant protein GFP, or Flag-RanBP9. Intriguingly, RanBP9 overexpressing cells showed a significant >2-fold increase in Hsp90 binding to ATP-agarose compared to vector or GFP control transfected cells, suggesting an increased capacity for Hsp90 complexes to bind ATP (Fig. 5A and B). We also performed ATP-

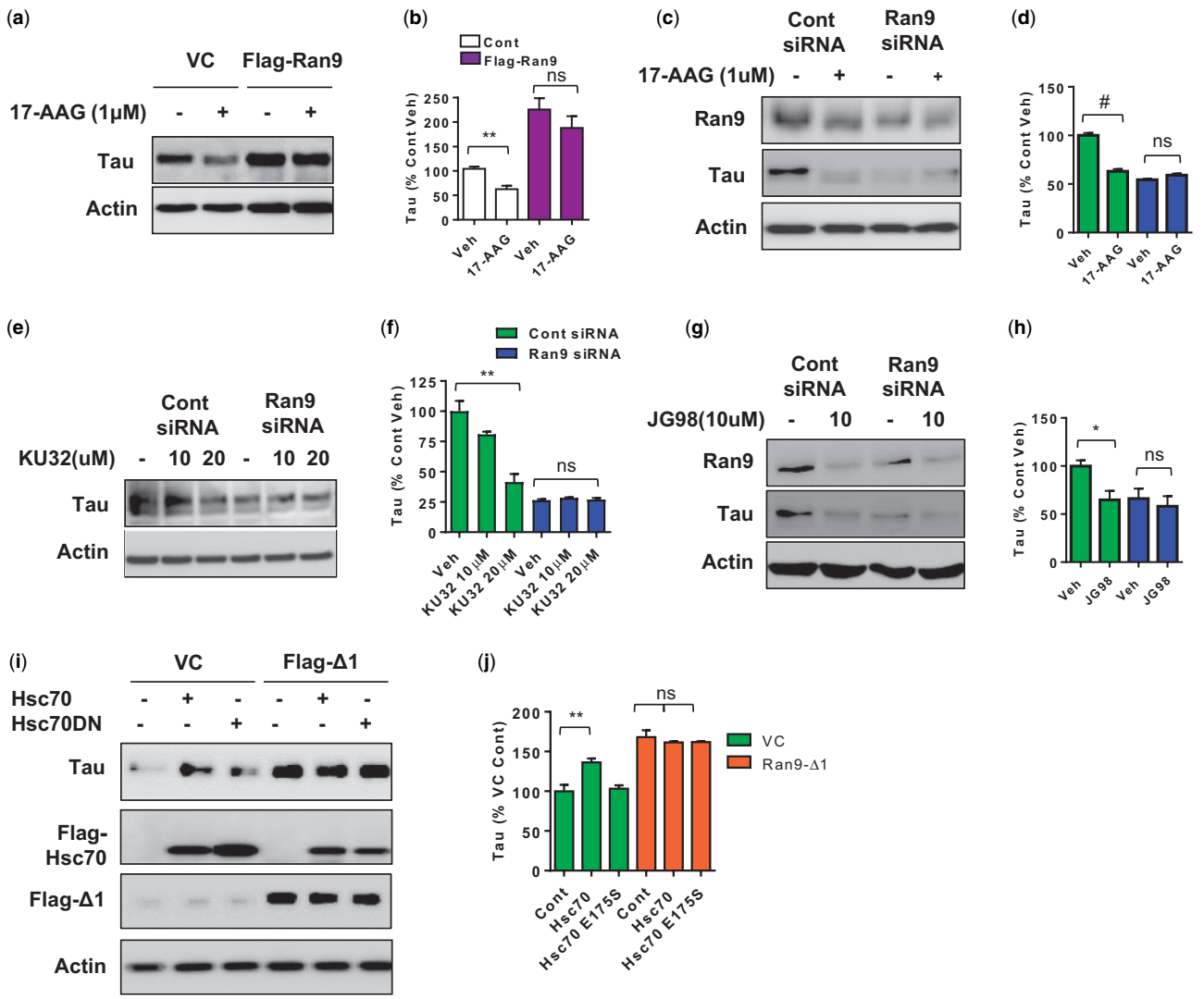


**Figure 4.** RanBP9 modulates the efficacy of Hsp90/Hsc70 inhibitors and Hsc70 variants. **(A,B)** Hela V5-Tau cells transfected with vector control or RanBP9, treated with 17-AAG (1 μM, 16 h), and subjected to immunoblotting for the indicated proteins. (B) Quantification of tau levels (t-test, veh vs. 17-AAG, $^{**}P < 0.005$, $n = 6$ replicates). **(C,D)** Hela-V5-Tau cells transfected with control or RanBP9 siRNA, treated with 17-AAG (1 μM, 16 h), and subjected to immunoblotting for the indicated proteins. **(D)** Quantification of tau levels (t-test, veh vs. 17-AAG, $^{\#}P < 0.0001$, $n = 4$ replicates). **(E,F)** Hela-V5-Tau cells transfected with control or RanBP9 siRNA, treated with different doses of KU-32 for 16 h, and subjected to immunoblotting for the indicated proteins. **(F)** Quantification of tau levels with different doses of KU-32 in control or RanBP9 siRNA transfected cells (ANOVA, veh vs. KU32, post hoc Tukey, $^{**}P < 0.005$, $n = 6$ replicates). **(G,H)** Hela-V5-Tau cells transfected with control or RanBP9 siRNA, treated with JG-98 (10 μM, 1 h), and subjected to immunoblotting for the indicated proteins. **(H)** Quantification of tau levels (t-test, veh vs. JG-98, $^{*}P < 0.05$, $n = 4$ replicates) **(I,J)** HelaV5-Tau cells transfected with vector control, Hsc70, and Hsc70-E175S (dominant negative, DN) with/without RanBP9-Δ1 and subjected to immunoblotting for the indicated proteins. **(J)** Quantification of tau levels (ANOVA, Cont vs. Hsc70 variants, post hoc Tukey, $^{**}P < 0.005$, $n = 6$ replicates). **(K,L)** DIV7 cortical primary neurons derived from WT, TauP301S, TauP301S;*RanBP9*+/− transduced with Hsc70 or Hsc70 DN and subjected to immunoblotting for the indicated proteins. **(L)** Quantification of tau levels (ANOVA, Cont vs. Hsc70 variants, post hoc Tukey, $^{\#}P < 0.0001$, $n = 4$ replicates/genotype). **(M,N)** WT and *RanBP9*−/− DIV7 hippocampal primary neurons transduced with Hsc70 or Hsc70 DN and subjected to immunocytochemistry for tau and MAP2. **(N)** Quantitation of tau intensity (ANOVA, Cont vs. Hsc70 variants, post hoc Tukey, $^{*}P < 0.05$, $^{**}P < 0.005$, $^{\#}P < 0.0001$, $n = 9$ replicates/genotype). **(O,P)** WT and *RanBP9*−/− DIV14 cortical primary neurons treated with/without JG98 and subjected to immunoblotting for RanBP9, tau, and actin. (ANOVA, Cont vs. JG98 (10 μM, 1 h), post hoc Tukey, $^{**}P < 0.005$, $n = 4$ replicates). **(Q,R)** WT and *RanBP9*−/− DIV14 cortical primary neurons treated with/without 17-AAG (10 μM, 16 h) and subjected to immunoblotting for RanBP9, tau, and actin. (ANOVA, Cont vs. 17-AAG, post hoc Tukey, $^{**}P < 0.005$, $n = 4$ replicates).

agarose pull-down for Hsc70. Indeed, RanBP9 overexpressing cells also showed a significant >2-fold increase of Hsc70 binding to ATP-agarose compared to vector or GFP control transfected cells (Fig. 5A and B).

Given the physical interaction of RanBP9 with Hsp90 and Hsc70 complexes and the robust increase in ATP-binding capacity of both Hsp90 and Hsc70 upon RanBP9 overexpression, we next tested whether RanBP9 affects ATPase activity of Hsc70 and Hsp90 *in vitro*. We first incubated recombinant Hsc70 together with/without recombinant RanBP9 (PSL domain) with varying concentrations of ATP and measured Hsc70 ATPase activity by malachite green assay. As expected, increasing ATP concentrations yielded increased ATPase activity in a saturating manner (Fig. 5C). Addition of RanBP9-PSL increased Hsc70 ATPase activity, especially at low ATP concentrations (125 & 250 μM) (Fig. 5C), and multiple experiments confirmed that RanBP9-PSL significantly increases Hsc70 ATPase activity by >60% at 125 μM ATP concentration *in vitro* (Fig. 5D). Similar

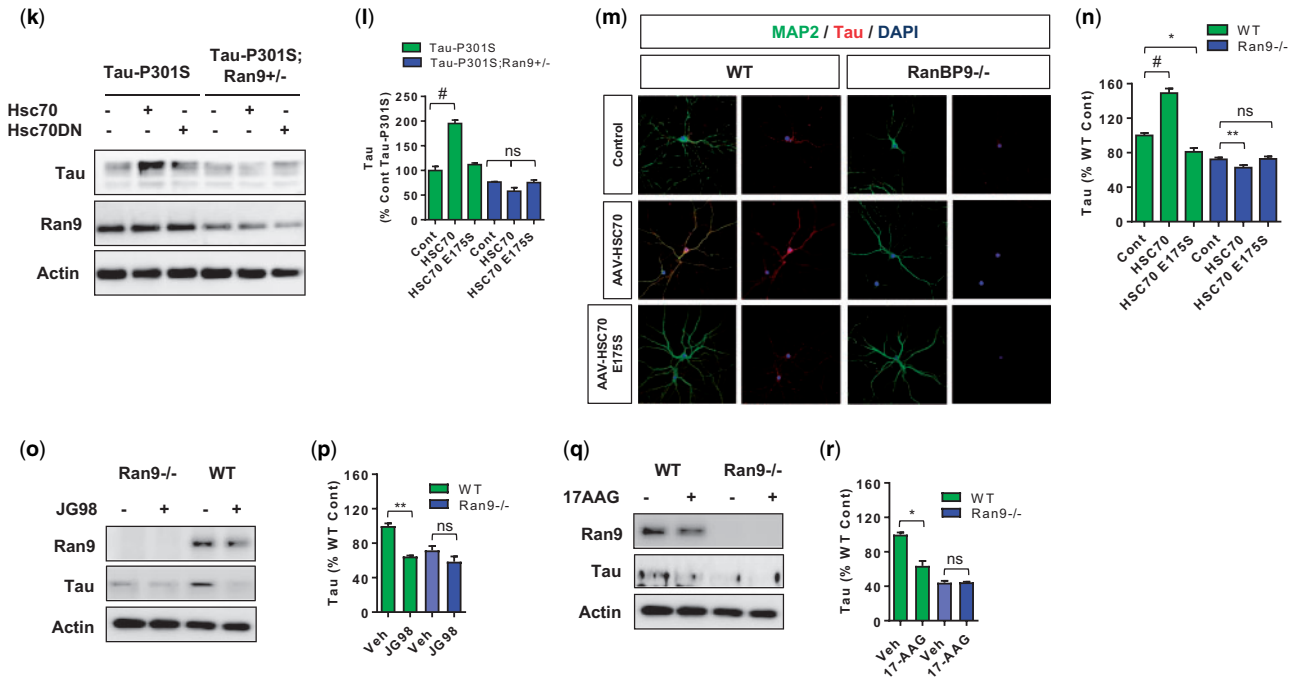


Figure 4. Continued

stimulation of Hsp90 ATPase activity by RanBP9-PSL was also seen (Fig. 5E), such that the addition of RanBP9-PSL enhanced Hsp90 activity by a significant 46% at 125 μM ATP concentration (Fig. 5E and F), whereas RanBP9-PSL *per se* contained no ATPase activity (Fig. 5E). These results therefore indicate that RanBP9 not only promotes ATP binding capacity of Hsp90/Hsc70 complexes but also directly enhances Hsc70 and Hsp90 ATPase activities to preserve tau, similar to chemical activators of Hsc70 activity (15).

## Genetic reduction in *RanBP9* ameliorates tau pathology in tau-P301S mice *in vivo*

We performed immunohistochemistry for human tau (HT7) in 6-month-old Tau-P301S and Tau-P301S;*RanBP9*+/– littermates brains. As expected, Tau-P301S;*RanBP9*+/– mice demonstrated significantly decreased HT7 (total human tau) immunoreactivity throughout the cortex compared to Tau-P301S littermates (Fig. 6A and B). Furthermore, we performed immunohistochemistry for pTau199/202 to detect phospho-tau at Serine 199/202 in the hippocampus and cortex of WT, Tau-P301S, and Tau-P301S;*RanBP9*+/– littermates. Indeed, p199/202 positive phospho-tau was dramatically increased in Tau-P301S hippocampus and cortex compared to WT mice (Fig. 6C and D). However, p199/202-tau was significantly decreased by ~75% in Tau-P301S;*RanBP9*+/– mice in both hippocampus and cortex compare to littermate Tau-P301S mice (Fig. 6C and D), similar to that seen with total tau (HT7). Immunoblotting and quantification of phospho-tau from the hippocampus confirmed that pTau199/202 and pTau396/404 (PHF-1) were indeed reduced in Tau-P301S;*RanBP9*+/– mice compared to Tau-P301S mice (Fig. 6E and F). As expected from the observed tauopathy in the Tau-P301S mice, GFAP-positive hippocampal astrogliosis was significantly increased in Tau-P301S mice compared to littermate WT mice (Fig. 6G and H). In contrast, Tau-P301S;*RanBP9*+/– hippocampus exhibited significantly reduced GFAP immunoreactivity to levels that were indistinguishable from WT littermate mice (Fig. 6G and H).

## *RanBP9* reduction rescues deficits in synaptic integrity and plasticity in tau-P301S mice

We next examined brains of 6-month-old Tau-P301S, Tau-P301S;*RanBP9*+/–, and WT littermates mice for synaptophysin immunoreactivity, a presynaptic marker. In the hippocampus, Tau-P301S mice demonstrated significantly decreased synaptophysin intensity within the stratum lucidium (SL: synaptic terminating zone) of hippocampal Cornus ammonis 3 (CA3) region (Fig. 7A and B). However, Tau-P301S;*RanBP9*+/– mice showed significantly restored synaptophysin intensity in the SL to levels that were indistinguishable from WT mice (Fig. 7A and B). To investigate synaptic integrity in a different way, we cultured P0 primary hippocampal neurons derived from WT, Tau-P301S, and Tau-P301S;*RanBP9*+/– littermates. Immunocytochemistry on DIV21 showed a significant depletion of drebrin, a postsynaptic marker, within primary dendrites and dendritic spines of Tau-P301S neurons compared to WT neurons (Fig. 7C and D). In contrast, drebrin fluorescence intensity in Tau-P301S;*RanBP9*+/– primary neurons was significantly restored nearly to levels seen in WT neurons (Fig. 7C and D).

To investigate the functional correlates of tauopathy and synaptic integrity in terms of changes in synaptic plasticity, we utilized acute hippocampal slices derived from 3-month old WT, Tau-P301S, and Tau-P301S;*RanBP9*+/– littermates, similar to our previous investigations of APP/PS1 mice (17). The simulating electrode was placed in the Schaffer collaterals of the hippocampus, and the recording electrode was positioned at the CA1 stratum radiatum below the pyramidal cell layer. Input-output analysis by stepping up the stimulus intensity from 0 to 15 mV showed no significant differences between WT and Tau-P301S

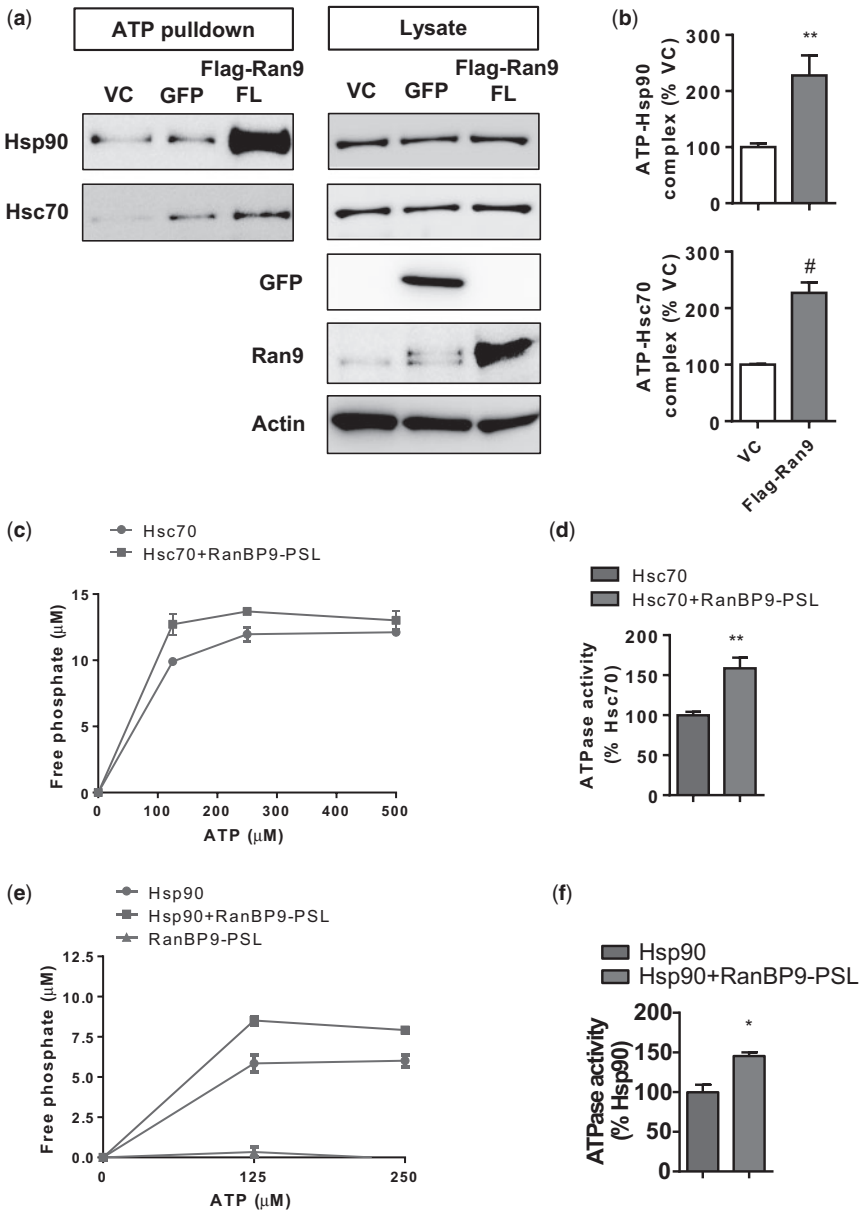


**Figure 5.** RanBP9 promotes Hsp90/Hsc70 ATP binding and directly enhances their ATPase activities. (**A,B**) Hela-V5-Tau cells transfected with vector control (VC), GFP or RanBP9, lysates pulled down with ATP beads, and immunoblotted for Hsp90 or Hsc70. Lysates also immunoblotted for Hsp90, Hsc70, RanBP9, GFP and actin. (B) Quantification of Hsp90 or Hsc70 pulled down by ATP beads (t-test, $^{**}P < 0.005$, $^{\#}P < 0.0001$, $n = 8$ replicates). (**C,D**) Recombinant Hsc70 ATPase activity malachite green assay conducted with/without recombinant RanBP9-PSL with the indicated concentrations of ATP for 2 h. (**D**) Quantification of Hsc70 ATPase activity with/without recombinant RanBP9-PSL normalized to Hsc70 alone (2 h, 125 μM ATP, t-test, $^{**}P < 0.005$, $n = 6$ replicates). (**E,F**) Recombinant Hsp90 ATPase activity malachite green assay conducted with/without recombinant RanBP9-PSL or RanBP9-PSL alone with indicated concentrations of ATP for 2 h. (**F**) Quantification of Hsp90 ATPase activity with/without recombinant RanBP9-PSL normalized to Hsp90 alone (2 h, 125 μM ATP, t-test, $^{*}P < 0.05$, $n = 4$ replicates).

slices or between Tau-P301S and Tau-P301S;*RanBP9*+/− slices, although a subtle but significant increase was seen in Tau-P301S;*RanBP9*+/− slices compared to WT slices from 10 to 15 mV (Fig. 7E). In paired pulse facilitation (PPF) studies, a significant decrease in fEPSP slope was seen in Tau-P301S slices compared to WT slices across the vast majority of interstimulus intervals, while no significances differences were seen between WT and Tau-P301S;*RanBP9*+/− slices (Fig. 7F). In long-term potentiation (LTP) experiments using theta burst stimulation, Tau-P301S slices exhibited severely defective induction and maintenance of LTP compared to WT and Tau-P301S;*RanBP9*+/− slices, while LTP in Tau-P301S;*RanBP9*+/− slices was essentially indistinguishable from that of WT slices (Fig. 7G). These data taken together demonstrate that endogenous RanBP9 levels are essential to promote tauopathy and associated deficits in synaptic plasticity.

## Discussion

In this study, we utilized a human cell line expressing human tau, primary neurons of various tau and *RanBP9* genotypes, acute brain slices, and genetically modified mice to investigate the role of RanBP9/Hsp90/Hsc70 complexes in tau level and

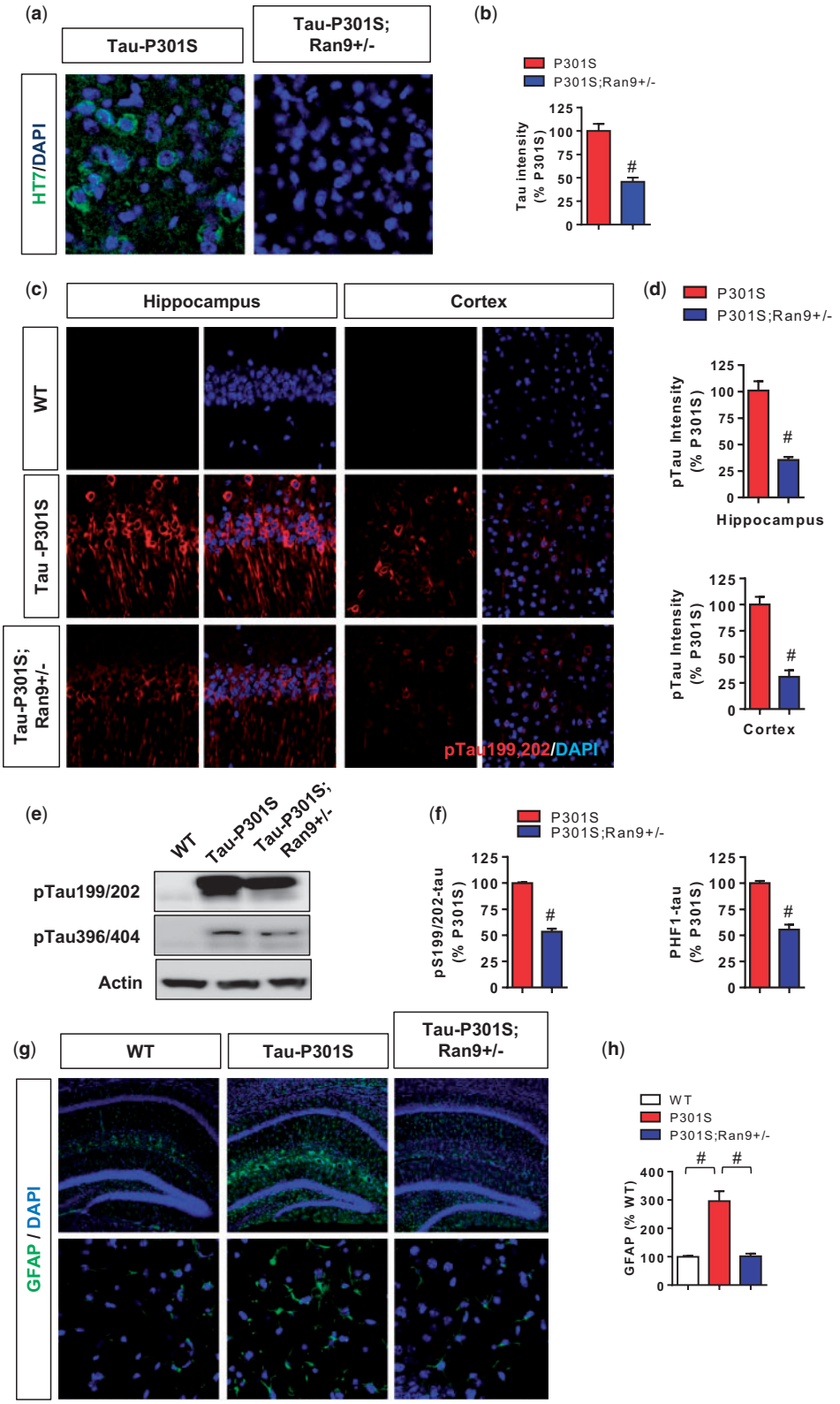


**Figure 6.** Genetic reduction of *RanBP9* rescues tauopathy and gliosis in Tau-P301S transgenic mice. **(A,B)** Six-month old Tau-P301S and Tau-P301S;*RanBP9*+/− littermate mice subjected to staining for total human tau (HT7 antibody). Representative images of HT7 staining in the anterior cortex shown. (B) Quantification of HT7 intensity in the anterior cortex of 6-month- old Tau-P301S and Tau-P301S;*RanBP9*+/− littermate mice (t-test, $^{\#}P < 0.0001$, $n = 6$ mice per genotype). **(C,D)** Brains from 6-month-old WT, Tau-P301S, and Tau-P301S;*RanBP9*+/− littermate mice subjected to immunohistochemistry for pTau199/202 (phospho-tau at Serine 199/202) in the hippocampus and cortex. Representative images shown. **d** Quantification of pTau199/202 intensity in the hippocampus (CA3) and anterior cortex (t-test, $^{\#}P < 0.0001$, $n = 6$ mice per genotype). **(E,F)** Brain hippocampi from 6-month-old WT, Tau-P301S, and Tau-P301S;*RanBP9*+/− littermate mice subjected to immunoblotting for pS199/202-tau and pS396/404-tau (PHF1). **(F)** Quantification of pS199/202-tau and pS396/404-tau levels (t-test, $^{\#}P < 0.0001$, $n = 6$ mice per genotype). **(G,H)** Brains from 6-month-old WT, Tau-P301S, and Tau-P301S;*RanBP9*+/− littermates stained for GFAP and DAPI. Representative images captured by 10X (upper) and 60X (lower) objectives shown. (H) Quantification of GFAP intensity in the hippocampus (1-way ANOVA, post hoc Tukey, $^{\#}P < 0.0001$, $n = 6$ mice per genotype).

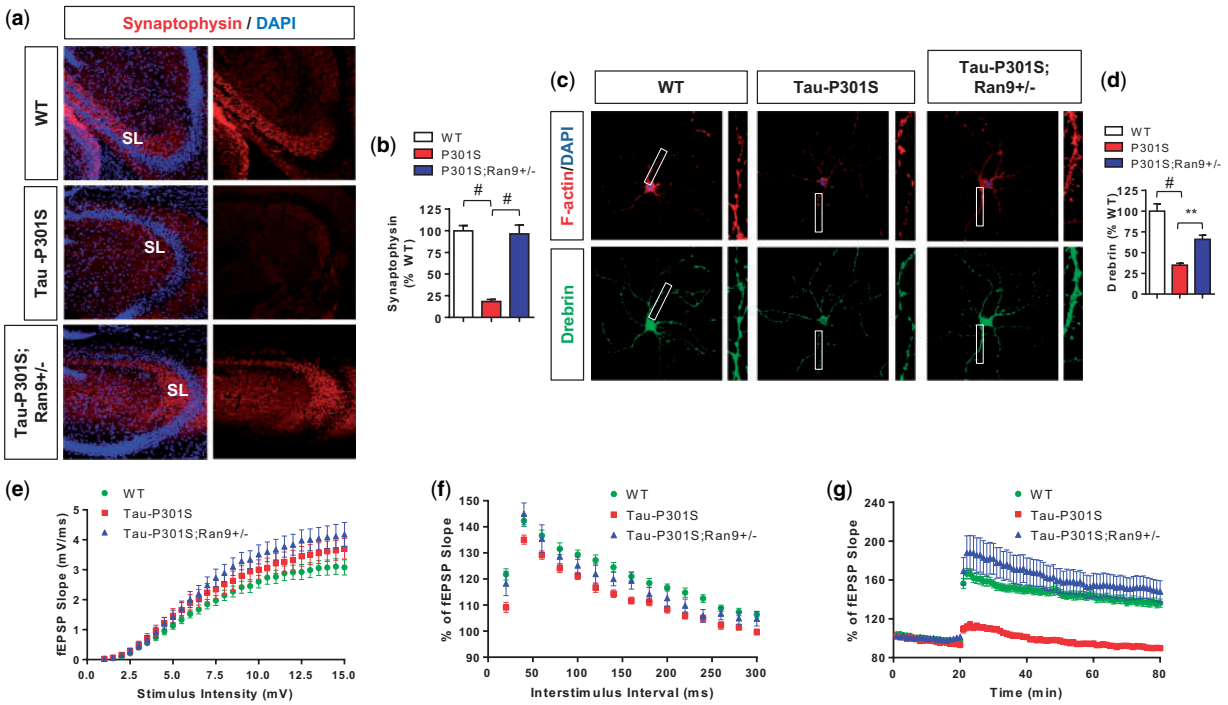


**Figure 7.** Genetic reduction in *RanBP9* rescues synaptic dysfunction in Tau-P301S transgenic mice. (**A,B**) Brains from 6-month-old WT, Tau-P301S, and Tau-P301S;*RanBP9*+/− littermates stained for synaptophysin and DAPI, showing representative hippocampus images captured by a 10X objective. (**B**) Quantification of synaptophysin intensity within the stratum lucidum (SL) of CA3 (1-way ANOVA, post hoc Tukey, $^{\#}P < 0.0001$, $n = 6$ mice per genotype). (**C,D**) DIV21 hippocampal neurons from WT, Tau-P301S, and Tau-P301S;*RanBP9*+/− littermate mice stained for F-actin (phalloidin) and drebrin. Representative images with magnified insets shown. (D) Quantification of mean drebrin intensity in spine-containing neurites (1-way ANOVA, post hoc Tukey, $^{**}P < 0.005$, $^{\#}P < 0.0001$, $n = 4$–6 replicates). (**E–G**) Stimulating electrode placed in the Schaffer collaterals of the hippocampus and recording glass electrode positioned at the CA1 stratum radiatum below the pyramidal cell layer. (E) Input/output (I/O) analysis generated by stepping up stimulation amplitude from 1 to 15 mV in WT, Tau-P301S, and Tau-P301S;*RanBP9*+/− acute slices. (2-way ANOVA, post hoc Tukey, significant differences between WT and Tau-P301S;*RanBP9*+/− from stimulus intensities 10 to 15 mV, $^{*}P < 0.05$ to $^{**}P < 0.005$, $n = 20$-45 slices/genotype from 3 to 4 mice/genotype). (F) PPF showing fEPSP slope as a function of 30-300 ms interstimulus interval (2-way ANOVA, post hoc Tukey, significant differences between WT and Tau-P301S at all interstimulus intervals, $^{*}P < 0.05$ to $^{***}P < 0.0001$, $n = 23$-49 slices/genotype from 3-4 mice/genotype). (G) LTP induced by theta burst stimulation showing significant differences in fEPSP slope between Tau-P301S compared to WT and Tau-P301S;*RanBP9*+/− slices (two-way ANOVA, post hoc Tukey, $^{***}P < 0.0001$ at all-time points following stimulation, $n = 22$-42 slices/genotype from 3-4 mice/genotype). All error bars represent S.E.M.

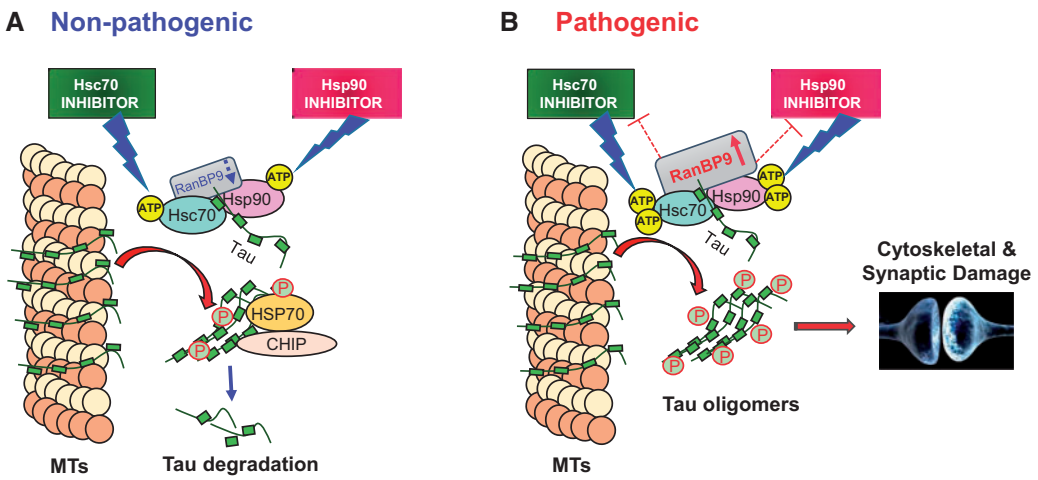


**Figure 8.** Schematic of RanBP9 action on tau via Hsp90/Hsc70 complexes. (**A**) Under non-pathogenic conditions where RanBP9 is at normal to moderate levels, Hsp90 and Hsc70 complexes normally triage tau upon decoupling from microtubules (MTs) for either degradation or preservation. Hsp90 and Hsc70 inhibitors under these conditions, trigger CHIP and proteasome-dependent degradation of misfolded tau. When RanBP9 decreases substantially under endogenous levels, a proportion of tau bypasses Hsp90/Hsc70 complexes and is directly routed for degradation. (**B**) Under pathogenic conditions where RanBP9 levels are aberrantly elevated (as in AD), the association of tau with Hsp90/Hsc70 complexes increases while simultaneously enhancing ATP binding to Hsp90/Hsc70 complexes, thereby disfavoring the tau degradation route. Under these conditions, the anti-tau potency of Hsp90 and Hsc70 inhibitors is reduced, thereby preserving misfolded tau.

tauopathy. We made a number of novel observations demonstrating that endogenous RanBP9, which we have previously shown to enhance Aβ production and mediate Aβ-induced neurotoxicity (17–19), also enhances tau levels *in vitro* and *in vivo*. Specifically, we showed for the first time that overexpression or knockdown of RanBP9 directly enhances and reduces tau level, respectively, *in vitro* and *in vivo*. Such changes in tau level were associated with the ability of RanBP9 to physically interact with tau and Hsp90/Hsc70 complexes. Meanwhile, both RanBP9 and tau levels were simultaneously reduced by Hsp90 and Hsc70 inhibitors, whereas overexpression or knockdown of RanBP9 significantly diminished the anti-tau potency of Hsp90/Hsc70 inhibitors as well as Hsc70 variants (WT & E175S), suggesting that RanBP9 alters the ability of Hsp90/Hsc70 complexes to triage and stabilize tau (Fig. 8). Indeed, we showed that RanBP9 increases the capacity for both Hsp90 and Hsc70 complexes to bind ATP and that the PSL domain of RanBP9 is sufficient to promote the ATPase activities of Hsp90 and Hsc70 *in vitro*. As both Hsp90 and Hsc70 are known to preferentially preserve tau upon decoupling from microtubules, our data indicate that the interaction of RanBP9 with Hsp90/Hsc70 complexes normally functions to facilitate this process (Fig. 8). These observations *in vitro* and cell lines were recapitulated in primary neurons and *in vivo*, as genetic reduction in *RanBP9* not only ameliorated tauopathy in Tau-P301S mice but also rescued the deficits in synaptic integrity and plasticity.

Tau is a microtubule associated protein that normally functions to stabilize microtubules (4). It has previously been shown that upon decoupling of tau from microtubules and hyperphosphorylation, chaperone proteins such as Hsp90 and Hsc70 complexes function to triage misfolded tau for degradation or refolding/preservation. The dominant activity of Hsp90 and Hsc70 on misfolded tau, however, appears to be the preservation of tau, since various specific Hsp90 and Hsc70 inhibitors result in the loss of tau via routing tau for proteasomal degradation. Our observation that RanBP9 interacts with both tau and Hsp90/Hsc70 complexes and promotes the complexation of tau with Hsp90 and Hsc70 is consistent with the notion that RanBP9 may function as scaffold upon which these proteins are assembled. This was also supported by the direct binding of RanBP9-PSL to tau and Hsc90/Hsc70 *in vitro*. Alternatively, but not mutually exclusively, it is plausible that RanBP9 alters the conformation of the Hsp90/Hsc70 complexes to facilitate tau/Hsp90/Hsc70 interaction in a way that does not readily permit the triaging of tau for degradation. The latter notion is supported by our observation that RanBP9 promotes ATP binding to both Hsp90 and Hsc70 complexes while enhancing their ATPase activities *in vitro*. To our knowledge, such protein-based regulatory activity of Hsp90/Hsc70 complexes on tau has not been observed before. Evidently, Hsp90 has been shown to have an increased affinity for ATP competitive inhibitors in AD brain tissue (9), suggesting a conformational change. Given that RanBP9 is elevated in AD and AD mouse model brains (16–18), the increased ATP binding of Hsp90 found here may be a contributing factor. At the same time, RanBP9 *per se* appears to be a client to the Hsp90/Hsc70 chaperone complex, while simultaneously assuming a regulatory function on the complex. Such mode of action may be needed to alternate rapidly between preservation or triaging of different client proteins in a normal physiological setting.

RanBP9 is a multi-domain scaffolding protein, which we and others have shown to affect multiple biochemical signaling processes (18,21,38–42). Complete loss of *RanBP9* leads to neonatal lethality associated with developmental patterning of the brain and other organs (38,43). However, we have also previously shown that genetic reduction in one copy of *RanBP9* blocks Aβ production and Aβ-induced neurotoxic changes (17–19). These *RanBP9*+/− mice are completely normal and viable. In this study, our findings indicated that reducing *RanBP9* also protects against tau pathology through a different mechanism. This mechanism involves Hsp90/Hsc70 complexes in a way to enhance the preservation of tau. Whether this phenomenon is unique to tau is unknown. However, we and others have shown that RanBP9 also stabilizes other proteins, such as SSH1, p73, and mgl-1 (17,42,44,45). In contrast, RanBP9 has also been implicated in destabilizing c-raf potentially by reducing its association with Hsp90 (26). Therefore, it is plausible to speculate that the effects of RanBP9 on Hsp90/Hsc70 complexes are varied depending on the client protein, leading to the facilitation of Hsp90/Hsc70 complexes binding to certain proteins (*i.e.* tau) at the expense of others (*i.e.* c-raf). Other studies have shown that RanBP9 is localized to various compartments in cells, including the plasma membrane associated with receptor complexes (21,46,47), cytoplasm associated with mitochondria and microtubules (44,48,49), and the nucleus associated with chromatin (49,50). As such, signal- and cell-dependent localization of RanBP9 will likely have differing effects on clients of Hsp90/Hsc70 complexes.

The observations that reducing *RanBP9* rescues amyloid, cofilin-actin, and tau pathologies (17) underscore the importance of RanBP9 as a unique and potentially viable therapeutic target for neurodegenerative diseases such as AD. We previously showed that the N-terminal 60-kD fragment of RanBP9 (RanBP9-Δ1) is dramatically increased in AD brains, and full-length RanBP9 is >3-fold increased in two different APP transgenic mouse models of amyloid pathology (J20 & APP/PS1) (16–18). Despite our observations that RanBP9 increases tau levels independent of its effect on Aβ production in our experimental setting, it is reasonable to postulate that increased RanBP9 levels in AD brains contribute to both elevated Aβ and tau levels. Moreover, as increased RanBP9 levels significantly nullified the potency of Hsp90/Hsc70 inhibitors on tau, and various Hsp90/Hsc70 inhibitors are currently being considered as potential therapeutic agents for AD (9,12,15,27,28,31), normalizing RanBP9 levels or activity may additionally prove to enhance the efficacy of Hsp90/Hsc70 inhibitors on neurodegenerative phenotypes.

## Materials and Methods

### Cells, constructs, siRNA sequences, and transfections

Stably transfected HeLa cells over-expressing wildtype 4R0N human tau (15), tet-regulated tau stable cell lines (51), Hsp90, Hsp90 D88N (36), Hsc70, Hsc70 E175S mutant constructs (52) have previously been described. The siRNA sequence targeting RanBP9 (5′-UCUUAUCAACAAUACCUGC-3′) was obtained from GE Dharmacon (Lafayette, CO, USA). All cells were transfected for 48 h using lipofectamine 2000 (Invitrogen, Carlsbad, CA, USA) per the manufacturer's instructions. Cortical and hippocampal neurons were derived from postnatal day 0 (P0) pups and cultured on poly-d-lysine-coated plates or coverslips as previously described (18,53). AAV9 was prepared according to standard methods (54,55). Primary neurons were transduced at DIV7 and harvested at DIV 15 or 18 for immunoblotting or at DIV21 for immunocytochemistry.

### Antibodies and reagents

Antibodies to total tau (TauH-150, Santa Cruz Biotechnology, Dallas, TX, USA), PHF1 (kind gift from Dr. Peter Davies, Albert

Einstein College of Medicine), pTau199/202 (Invitrogen, Carlsbad, CA, USA), HT7 (Invitrogen), GFAP (Invitrogen), synaptophysin (Invitrogen), Drebrin (Abcam, Cambridge, MA, USA), MAP2 (EMD Millipore, Billerica, MA, USA), Hsp90 (Stressgen Biotechnologies, Ann Arbor, MI, USA), Hsc70 (Stressgen, Enzo Life Sciences, Farmingdale, NY, USA), M2-Flag (Sigma-Aldrich, St. Louis, MO, USA), actin (Sigma-Aldrich), HRP-linked secondary antibodies (Jackson ImmunoResearch, West Grove, PA, USA), and fluorescently labeled secondary antibodies (Invitrogen) were obtained from the indicated sources. 17-AAG were acquired from A.G. Scientific (San Diego, CA, USA). JG-98 was a generous gift from Jason Gestwicki (UCSF), and KU-32 was a generous gift from Brian Blagg (University of Kansas).

## Cell/tissue lysis and immunoblotting

Cultured cells or brain (36) homogenates were lysed with lysis buffer (50 mM Tris-Cl, 150 mM NaCl, 2 mM EDTA, and 1% Triton X-100) unless stated otherwise. Total protein concentrations were quantified by the micro-BCA colorimetric protein detection assay (Pierce, Waltham, MA, USA). Equal amounts of protein were subjected to SDS-PAGE and transferred to nitrocellulose membranes for immunoblotting. Membranes were blocked for 1 h in 5% skim-milk in TBS-T before being incubated with primary antibodies. After probing with the primary antibodies, the corresponding peroxidase-conjugated secondary antibodies were detected by ECL (Merck Millipore, Darmstadt, Germany) and capture using the LAS-4000 imager (GE Healthcare Biosciences, Pittsburgh, PA).

## Quantitative real time RT–PCR

Quantitative real-time RT-PCR was performed using Roche LightCycler® 96 System (Life Science, San Francisco, CA, USA), following the manufacturer's recommended conditions. Total RNA was isolated from transiently transfected cells using Trizol reagent (Invitrogen), reverse transcribed (Superscript III, Invitrogen), and subjected to quantitative PCR analysis using Syber green master mix (Invitrogen). The comparative threshold cycle (Ct) value was used to calculate the amplification factor, and the relative level of target was normalized to GAPDH levels as we previously described (44). The primers sequences are as follows: Human Tau-forward 5'-CCAAGCTCGCATGGTCAGTA-3' and reverse-5'-GGCAGACACCTCGTCAGCTA-3'; mouse Tau-forward 5'-GGCTCTACTGAGAACCTGAA-3' and reverse 5'-TCTG CTCCATGGTCTGTCTT-3'; human GAPDH-forward 5'-AAGGT CGGAGTCAACGGATT-3' and reverse 5'-CCATGGGTGGAATCAT ATTGG-3'; Mouse GAPDH-forward 5'-TCAACAGCAACTCCCAC TCTT-3' and reverse 5'-ACCCTGTTGCTGTAGCCGTAT-3'.

## Recombinant protein binding and ATPase activity assays

Recombinant human Hsc70 or Hsp90 was used in a malachite green assay with or without recombinant RanBP9 (PSL domains, residues 147-397). A master mix of Hsc70 or Hsp90 was prepared in assay buffer (0.017% Triton X-100, 100 mM Tris – HCl, 20 mM KCl, and 6 mM MgCl2, pH 7.4). An aliquot of this mixture (10 µl) was added into each well of a 96-well plate. To this solution, RanBP9 and $H_2O$ were added to 36 µl, and the plate was incubated for 30 min at 25 °C before adding 4 µl of 10 mM ATP to start the reaction. Thus, the final reaction volume was 40 µl containing 1.25 µM Hsc70, ± 1 µM RanBP9, 0.017% Triton X-100, and varying concentrations ATP (or 0.125, 0.25, 0.5 mM). After 1 h of incubation at 37 °C, 80 µl of malachite green reagent was added into each well. The samples were mixed thoroughly and incubated at 25 °C for 30 min before measuring OD620. Phosphate standards (0–100 µM) were included in each experiment. Background ATP alone values were subtracted prior to analysis. For recombinant protein binding assays, combinations of indicated recombinant proteins were co-incubated for 16 h at 4 °C in binding buffer (50 mM Tris-Cl, pH 7.4, 150 mM NaCl, 0.1% triton X-100), and pulled down with the indicated antibodies plus IgG beads or IgG beads alone. Beads were washed at least three times in binding buffer prior to SDS-PAGE.

## Mice

Tau-P301S, WT, *RanBP9*+/– mice were all bred in the C57BL6 background for at least three generation prior to interbreeding with each other. Tau-P301S mice express mutant human tau-P301S driven by the mouse prion protein promoter (24). The *RanBP9*+/– mice have previously been characterized (17). Mice were supplied with water and food *ad libitum* with 12-h light/dark cycle at standard vivarium conditions.

## Immunofluorescence

Immunocytochemistry and Immunohistochemistry were performed as previously described (17,53). Briefly, animals were perfused with 4% paraformaldehyde in PBS. Later, brains were post-fixed in 4% paraformaldehyde in PBS for overnight, then cryoprotected in 30% sucrose and sectioned on a cryostat or microtome. For immunocytochemistry, cells were fixed in 4% paraformaldehyde in PBS for 15 min and blocked with 3% normal goat serum. Primary antibodies were applied for overnight at 4 °C, and secondary antibodies were applied for 45 min at room temperature. All images were acquired with the Olympus FV10i confocal microscope (Tokyo, Japan) and quantitated using the Image J software. Comparison images were acquired with identical laser intensity, exposure time, and filter. Adjustments to the brightness/contrast were applied equally to all comparison images. Regions of interest were chosen randomly, and investigators were blinded to experimental conditions during image acquisition and quantification.

## Electrophysiology

Electrophysiological recording was performed as previously described (53). Briefly, hippocampus slices were prepared from 3-month-old WT, Tau-P301S, and Tau-P301S;*RanBP9*+/– mice and subjected to input/output (IO) curve, PPF, and long-term potentiation (LTP) (56). The hippocampus was dissected and acclimated in 50:50 solution (cutting:artificial cerebrospinal fluid (ACSF) for 10 min at room temperature. Then the slices were transferred to ACSF (125 mM NaCl, 2.5 mM KCl, 1.25 mM $NaH_2PO_4$, 0.26 mM $NaHCO_3$, 1.2 mM $MgCl_2$, 2.0 mM $CaCl_2$, and 10 g/l glucose, pH 7.3–7.4, saturated with 95% $O_2$ and 5% $CO_2$). Slices were recovered in ACSF at room temperature at least 40 min, followed by a final incubation in ACSF for 1 h at 30 °C. Extracellular field potential recording, LTP: the recording chamber was held at 30 ± 0.5 °C with ACSF flow rate of 1 ml/min. The stimulating electrode was placed in the Schaffer collaterals of the hippocampus. The recording glass electrode loaded with ACSF was positioned at the CA1 stratum radiatum below the pyramidal cell layer.

### Statistical analysis and graphs

Statistical analyses were performed by the GraphPad Prism 6.0 software (GraphPad Software, San Diego, CA, USA) using Student's *t*-test, one- or two-way ANOVA. One- or two-way ANOVA was followed by the indicated *post hoc* tests. All quantitative graphs with error bars were expressed as mean ± S.E.M.

### Declarations

All experiments involving mice were performed in accordance with approved protocols by the Institutional Animal Care and Use Committee (IACUC) at USF Health.

## Supplementary Material

Supplementary Material is available at *HMG* online.

## Acknowledgements

We thank Drs. Laura Blair and John Koren for their helpful discussion (Dickey lab).

*Conflict of Interest statement*. None declared.

## Funding

Veterans Administration (VA) (1 I01 BX002478-01A1, D.E.K.), National Institutes of Health (NIH) (1R01AG053060-01A1 & 1R21AG050284-01, D.E.K.), Florida Department of Health (5AZ07, D.E.K.), and NIH/National Institute of Neurological Disorders and Stroke (NINDS) (5R01NS073899-07, D.E.K./C.A.D.).

## References

1. Morris, M., Maeda, S., Vossel, K. and Mucke, L. (2011) The many faces of tau. *Neuron*, **70**, 410–426.
2. Vossel, K.A., Zhang, K., Brodbeck, J., Daub, A.C., Sharma, P., Finkbeiner, S., Cui, B. and Mucke, L. (2010) Tau reduction prevents Abeta-induced defects in axonal transport. *Science*, **330**, 198.
3. Vossel, K.A., Xu, J.C., Fomenko, V., Miyamoto, T., Suberbielle, E., Knox, J.A., Ho, K., Kim, D.H., Yu, G.Q. and Mucke, L. (2015) Tau reduction prevents Abeta-induced axonal transport deficits by blocking activation of GSK3beta. *J. Cell Biol.*, **209**, 419–433.
4. Mandelkow, E.M., Biernat, J., Drewes, G., Gustke, N., Trinczek, B. and Mandelkow, E. (1995) Tau domains, phosphorylation, and interactions with microtubules. *Neurobiol. Aging*, **16**, 355–362. discussion 362-353.
5. Mandelkow, E.M. and Mandelkow, E. (2012) Biochemistry and cell biology of tau protein in neurofibrillary degeneration. *Cold Spring Harb. Perspect. Med.*, **2**, a006247.
6. Takalo, M., Salminen, A., Soininen, H., Hiltunen, M. and Haapasalo, A. (2013) Protein aggregation and degradation mechanisms in neurodegenerative diseases. *Am. J. Neurodegener. Dis.*, **2**, 1–14.
7. Dou, F., Netzer, W.J., Tanemura, K., Li, F., Hartl, F.U., Takashima, A., Gouras, G.K., Greengard, P. and Xu, H. (2003) Chaperones increase association of tau protein with microtubules. *Proc. Natl. Acad. Sci. U.S.A*, **100**, 721–726.
8. Blair, L.J., Nordhues, B.A., Hill, S.E., Scaglione, K.M., O'Leary, J.C., 3rd, Fontaine, S.N., Breydo, L., Zhang, B., Li, P., Wang, L. *et al.* (2013) Accelerated neurodegeneration through chaperone-mediated oligomerization of tau. *J. Clin. Invest.*, **123**, 4158–4169.
9. Dickey, C.A., Kamal, A., Lundgren, K., Klosak, N., Bailey, R.M., Dunmore, J., Ash, P., Shoraka, S., Zlatkovic, J., Eckman, C.B. *et al.* (2007) The high-affinity HSP90-CHIP complex recognizes and selectively degrades phosphorylated tau client proteins. *J. Clin. Invest.*, **117**, 648–658.
10. Jinwal, U.K., O'Leary, J.C., 3rd, Borysov, S.I., Jones, J.R., Li, Q., Koren, J., 3rd, Abisambra, J.F., Vestal, G.D., Lawson, L.Y., Johnson, A.G. *et al.* (2010) Hsc70 rapidly engages tau after microtubule destabilization. *J. Biol. Chem.*, **285**, 16798–16805.
11. Fontaine, S.N., Martin, M.D., Akoury, E., Assimon, V.A., Borysov, S., Nordhues, B.A., Sabbagh, J.J., Cockman, M., Gestwicki, J.E., Zweckstetter, M. *et al.* (2015) The active Hsc70/tau complex can be exploited to enhance tau turnover without damaging microtubule dynamics. *Hum. Mol. Genet.*, **24**, 3971–3981.
12. Luo, W., Dou, F., Rodina, A., Chip, S., Kim, J., Zhao, Q., Moulick, K., Aguirre, J., Wu, N., Greengard, P. *et al.* (2007) Roles of heat-shock protein 90 in maintaining and facilitating the neurodegenerative phenotype in tauopathies. *Proc. Natl. Acad. Sci. U.S.A*, **104**, 9511–9516.
13. Abisambra, J., Jinwal, U.K., Miyata, Y., Rogers, J., Blair, L., Li, X., Seguin, S.P., Wang, L., Jin, Y., Bacon, J. *et al.* (2013) Allosteric heat shock protein 70 inhibitors rapidly rescue synaptic plasticity deficits by reducing aberrant tau. *Biol. Psychiatry*, **74**, 367–374.
14. Jinwal, U.K., Akoury, E., Abisambra, J.F., O'Leary, J.C., 3rd, Thompson, A.D., Blair, L.J., Jin, Y., Bacon, J., Nordhues, B.A., Cockman, M. *et al.* (2013) Imbalance of Hsp70 family variants fosters tau accumulation. *FASEB J.*, **27**, 1450–1459.
15. Jinwal, U.K., Miyata, Y., Koren, J., 3rd, Jones, J.R., Trotter, J.H., Chang, L., O'Leary, J., Morgan, D., Lee, D.C., Shults, C.L. *et al.* (2009) Chemical manipulation of hsp70 ATPase activity regulates tau stability. *J. Neurosci.*, **29**, 12079–12088.
16. Lakshmana, M.K., Chung, J.Y., Wickramarachchi, S., Tak, E., Bianchi, E., Koo, E.H. and Kang, D.E. (2010) A fragment of the scaffolding protein RanBP9 is increased in Alzheimer's disease brains and strongly potentiates amyloid-beta peptide generation. *faseb J.*, **24**, 119–127.
17. Woo, J.A., Boggess, T., Uhlar, C., Wang, X., Khan, H., Cappos, G., Joly-Amado, A., De Narvaez, E., Majid, S., Minamide, L.S. *et al.* (2015) RanBP9 at the intersection between cofilin and Abeta pathologies: rescue of neurodegenerative changes by RanBP9 reduction. *Cell Death Dis.*, **6**, 1676.
18. Woo, J.A., Jung, A.R., Lakshmana, M.K., Bedrossian, A., Lim, Y., Bu, J.H., Park, S.A., Koo, E.H., Mook-Jung, I. and Kang, D.E. (2012) Pivotal role of the RanBP9-cofilin pathway in Abeta-induced apoptosis and neurodegeneration. *Cell Death Differ.*, **19**, 1413–1423.
19. Lakshmana, M.K., Yoon, I.S., Chen, E., Bianchi, E., Koo, E.H. and Kang, D.E. (2009) Novel role of RanBP9 in BACE1 processing of amyloid precursor protein and amyloid beta peptide generation. *J.Biol.Chem.*, **284**, 11863–11872.
20. Lakshmana, M.K., Hayes, C.D., Bennett, S.P., Bianchi, E., Reddy, K.M., Koo, E.H. and Kang, D.E. (2012) Role of RanBP9 on amyloidogenic processing of APP and synaptic protein levels in the mouse brain. *faseb J.*, **26**, 2072–2083.
21. Woo, J.A., Roh, S.E., Lakshmana, M.K. and Kang, D.E. (2012) Pivotal role of RanBP9 in integrin-dependent focal adhesion signaling and assembly. *faseb J.*, **26**, 1672–1681.
22. Rapoport, M., Dawson, H.N., Binder, L.I., Vitek, M.P. and Ferreira, A. (2002) Tau is essential to beta -amyloid-induced neurotoxicity. *Proc. Natl. Acad. Sci. U.S.A*, **99**, 6364–6369.

23. Jin, M., Shepardson, N., Yang, T., Chen, G., Walsh, D. and Selkoe, D.J. (2011) Soluble amyloid {beta}-protein dimers isolated from Alzheimer cortex directly induce Tau hyperphosphorylation and neuritic degeneration. *Proc. Natl. Acad.Sci. U.S.A*, **108**, 5819–5824.
24. Yoshiyama, Y., Higuchi, M., Zhang, B., Huang, S.M., Iwata, N., Saido, T.C., Maeda, J., Suhara, T., Trojanowski, J.Q. and Lee, V.M. (2007) Synapse loss and microglial activation precede tangles in a P301S tauopathy mouse model. *Neuron*, **53**, 337–351.
25. Nishitani, H., Hirose, E., Uchimura, Y., Nakamura, M., Umeda, M., Nishii, K., Mori, N. and Nishimoto, T. (2001) Full-sized RanBPM cDNA encodes a protein possessing a long stretch of proline and glutamine within the N-terminal region, comprising a large protein complex. *Gene*, **272**, 25–33.
26. Atabakhsh, E. and Schild-Poulter, C. (2012) RanBPM is an inhibitor of ERK signaling. *PloS One*, **7**, e47803.
27. Dickey, C.A., Eriksen, J., Kamal, A., Burrows, F., Kasibhatla, S., Eckman, C.B., Hutton, M. and Petrucelli, L. (2005) Development of a high throughput drug screening assay for the detection of changes in tau levels – proof of concept with HSP90 inhibitors. *Curr. Alzheimer Res.*, **2**, 231–238.
28. Dickey, C.A., Ash, P., Klosak, N., Lee, W.C., Petrucelli, L., Hutton, M. and Eckman, C.B. (2006) Pharmacologic reductions of total tau levels; implications for the role of microtubule dynamics in regulating tau expression. *Mol. Neurodegener.*, **1**, 6.
29. Shimura, H., Schwartz, D., Gygi, S.P. and Kosik, K.S. (2004) CHIP-Hsc70 complex ubiquitinates phosphorylated tau and enhances cell survival. *J. Biol. Chem.*, **279**, 4869–4876.
30. Thompson, A.D., Scaglione, K.M., Prensner, J., Gillies, A.T., Chinnaiyan, A., Paulson, H.L., Jinwal, U.K., Dickey, C.A. and Gestwicki, J.E. (2012) Analysis of the tau-associated proteome reveals that exchange of Hsp70 for Hsp90 is involved in tau degradation. *ACS Chem. Biol.*, **7**, 1677–1686.
31. Ho, S.W., Tsui, Y.T., Wong, T.T., Cheung, S.K., Goggins, W.B., Yi, L.M., Cheng, K.K. and Baum, L. (2013) Effects of 17-allylamino-17-demethoxygeldanamycin (17-AAG) in transgenic mouse models of frontotemporal lobar degeneration and Alzheimer's disease. *Transl. Neurodegener.*, **2**, 24.
32. Hadden, M.K., Hill, S.A., Davenport, J., Matts, R.L. and Blagg, B.S. (2009) Synthesis and evaluation of Hsp90 inhibitors that contain the 1,4-naphthoquinone scaffold. *Bioorg. Med. Chem.*, **17**, 634–640.
33. Li, X., Shao, H., Taylor, I.R. and Gestwicki, J.E. (2016) Targeting Allosteric Control Mechanisms in Heat Shock Protein 70 (Hsp70). *Curr. Top. Med. Chem.*, **16**, 2729–2740.
34. Miyata, Y., Li, X., Lee, H.F., Jinwal, U.K., Srinivasan, S.R., Seguin, S.P., Young, Z.T., Brodsky, J.L., Dickey, C.A., Sun, D. *et al.* (2013) Synthesis and initial evaluation of YM-08, a blood-brain barrier permeable derivative of the heat shock protein 70 (Hsp70) inhibitor MKT-077, which reduces tau levels. *ACS Chem. Neurosci.*, **4**, 930–939.
35. Rousaki, A., Miyata, Y., Jinwal, U.K., Dickey, C.A., Gestwicki, J.E. and Zuiderweg, E.R. (2011) Allosteric drugs: the interaction of antitumor compound MKT-077 with human Hsp70 chaperones. *J. Mol. Biol.*, **411**, 614–632.
36. Miao, R.Q., Fontana, J., Fulton, D., Lin, M.I., Harrison, K.D. and Sessa, W.C. (2008) Dominant-negative Hsp90 reduces VEGF-stimulated nitric oxide release and migration in endothelial cells. *Arterioscler. Thromb. Vasc. Biol.*, **28**, 105–111.
37. Fontaine, S.N., Zheng, D., Sabbagh, J.J., Martin, M.D., Chaput, D., Darling, A., Trotter, J.H., Stothert, A.R., Nordhues, B.A., Lussier, A. *et al.* (2016) DnaJ/Hsc70 chaperone complexes control the extracellular release of neurodegenerative-associated proteins. *EMBO J.*, **35**, 1537–1549.
38. Bao, J., Tang, C., Li, J., Zhang, Y., Bhetwal, B.P., Zheng, H. and Yan, W. (2014) RAN-binding protein 9 is involved in alternative splicing and is critical for male germ cell development and male fertility. *PLoS Genet.*, **10**, e1004825.
39. Wei, J.D., Kim, J.Y., Kim, A.K., Jang, S.K. and Kim, J.H. (2013) RanBPM protein acts as a negative regulator of BLT2 receptor to attenuate BLT2-mediated cell motility. *J. Biol. Chem.*, **288**, 26753–26763.
40. Atabakhsh, E., Bryce, D.M., Lefebvre, K.J. and Schild-Poulter, C. (2009) RanBPM has proapoptotic activities that regulate cell death pathways in response to DNA damage. *Mol. Cancer Res.*, **7**, 1962–1972.
41. Valiyaveettil, M., Bentley, A.A., Gursahaney, P., Hussien, R., Chakravarti, R., Kureishy, N., Prag, S. and Adams, J.C. (2008) Novel role of the muskelin-RanBP9 complex as a nucleocytoplasmic mediator of cell morphology regulation. *J. Cell Biol.*, **182**, 727–739.
42. Kramer, S., Ozaki, T., Miyazaki, K., Kato, C., Hanamoto, T. and Nakagawara, A. (2005) Protein stability and function of p73 are modulated by a physical interaction with RanBPM in mammalian cultured cells. *Oncogene*, **24**, 938–944.
43. Palavicini, J.P., Lloyd, B.N., Hayes, C.D., Bianchi, E., Kang, D.E., Dawson-Scully, K. and Lakshmana, M.K. (2013) RanBP9 Plays a Critical Role in Neonatal Brain Development in Mice. *PloS One*, **8**, e66908.
44. Liu, T., Roh, S.E., Woo, J.A., Ryu, H. and Kang, D.E. (2013) Cooperative role of RanBP9 and P73 in mitochondria-mediated apoptosis. *Cell Death Dis.*, **4**, e476.
45. Hong, S.K., Kim, K.H., Song, E.J. and Kim, E.E. (2016) Structural basis for the interaction between the IUS-SPRY domain of RanBPM and DDX-4 in germ cell development. *J. Mol. Biol.*, **428**, 4330–4344.
46. Zhang, J., Ma, W., Tian, S., Fan, Z., Ma, X., Yang, X., Zhao, Q., Tan, K., Chen, H., Chen, D. *et al.* (2014) RanBPM interacts with TbetaRI, TRAF6 and curbs TGF induced nuclear accumulation of TbetaRI. *Cell. Signal.*, **26**, 162–172.
47. Togashi, H., Schmidt, E.F. and Strittmatter, S.M. (2006) RanBPM contributes to Semaphorin3A signaling through plexin-A receptors. *J. Neurosci.*, **26**, 4961–4969.
48. Roh, S.E., Woo, J.A., Lakshmana, M.K., Uhlar, C., Ankala, V., Boggess, T., Liu, T., Hong, Y.H., Mook-Jung, I., Kim, S.J. *et al.* (2013) Mitochondrial dysfunction and calcium deregulation by the RanBP9-cofilin pathway. *faseb J.*, **27**, 4776–4789.
49. Salemi, L.M., Loureiro, S.O. and Schild-Poulter, C. (2015) Characterization of RanBPM molecular determinants that control its subcellular localization. *PloS One*, **10**, e0117655.
50. Domingues, S.C., Konietzko, U., Henriques, A.G., Rebelo, S., Fardilha, M., Nishitani, H., Nitsch, R.M., da Cruz, E.S.E.F. and da Cruz, E.S.O.A. (2014) RanBP9 modulates AICD localization and transcriptional activity via direct interaction with Tip60. *J. Alzheimer's Dis.*, **42**, 1415–1433.
51. Abisambra, J.F., Jinwal, U.K., Blair, L.J., O'Leary, J.C., 3rd, Li, Q., Brady, S., Wang, L., Guidi, C.E., Zhang, B., Nordhues, B.A. *et al.* (2013) Tau accumulation activates the unfolded protein response by impairing endoplasmic reticulum-associated degradation. *J. Neurosci.*, **33**, 9498–9507.
52. Fontaine, S.N., Rauch, J.N., Nordhues, B.A., Assimon, V.A., Stothert, A.R., Jinwal, U.K., Sabbagh, J.J., Chang, L., Stevens, S.M., Jr., Zuiderweg, E.R. *et al.* (2015) Isoform-selective genetic inhibition of constitutive cytosolic Hsp70 activity promotes

client Tau degradation using an altered co-chaperone complement. *J. Biol. Chem.*, **290**, 13115–13127.
53. Woo, J.A., Zhao, X., Khan, H., Penn, C., Wang, X., Joly-Amado, A., Weeber, E., Morgan, D. and Kang, D.E. (2015) Slingshot-Cofilin activation mediates mitochondrial and synaptic dysfunction via Abeta ligation to beta1-integrin conformers. *Cell Death Differ.*, **22**, 1069–1070.
54. Reiser, M. and Zolotukhin, S. (1999) Construction of Recombinant Adeno-Associated Virus (AAV). *Methods Mol. Med.*, **19**, 533–538.
55. Carty, N., Lee, D., Dickey, C., Ceballos-Diaz, C., Jansen-West, K., Golde, T.E., Gordon, M.N., Morgan, D. and Nash, K. (2010) Convection-enhanced delivery and systemic mannitol increase gene product distribution of AAV vectors 5, 8, and 9 and increase gene product in the adult mouse brain. *J. Neurosci. Methods*, **194**, 144–153.
56. Weeber, E.J., Beffert, U., Jones, C., Christian, J.M., Forster, E., Sweatt, J.D. and Herz, J. (2002) Reelin and ApoE receptors cooperate to enhance hippocampal synaptic plasticity and learning. *J. Biol. Chem.*, **277**, 39944–39952.